Optimized tomography of continuous variable systems using excitation counting

Chao Shen, Reinier W. Heeres, Philip Reinhold, Luyao Jiang, Yi-Kai Liu, Robert J. Schoelkopf, and Liang Jiang

Optimized Tomography of Continuous Variable Systems Using Excitation Counting

Chao Shen,[1] Reinier W. Heeres,[1] Philip Reinhold,[1] Luyao Jiang,[2]
Yi-Kai Liu,[3, 4] Robert J. Schoelkopf,[1] and Liang Jiang[1]

[1]*Department of Applied Physics, Yale University, New Haven, CT 06511, USA*
[2]*Department of Physics, Yale University, New Haven, CT 06511, USA*
[3]*Joint Center for Quantum Information and Computer Science (QuICS),*
University of Maryland, College Park, MD 20742, USA
[4]*National Institute of Standards and Technology (NIST), Gaithersburg, MD 20899, USA*

We propose a systematic procedure to optimize quantum state tomography protocols for continuous variable systems based on excitation counting preceded by a displacement operation. Compared with conventional tomography based on Husimi or Wigner function measurement, the excitation counting approach can significantly reduce the number of measurement settings. We investigate both informational completeness and robustness, and provide a bound of reconstruction error involving the condition number of the sensing map. We also identify the measurement settings that optimize this error bound, and demonstrate that the improved reconstruction robustness can lead to an order of magnitude reduction of estimation error with given resources. This optimization procedure is general and can incorporate prior information of the unknown state to further simplify the protocol.

I. INTRODUCTION

Quantum state tomography (QST) is a powerful procedure to completely characterize quantum states, which can be extended to quantum process tomography for general quantum operations. However, QST is often resource-consuming, involving preparation of a large number of identical unknown states and measurement of a large set of independent observables. For qubit systems, many techniques have been developed to reduce the cost of full state tomography, such as compressed sensing [1–3], permutationally invariant tomography [4], self-guided/adaptive tomography [5, 6], matrix product states tomography [7]. In contrast, for continuous variable (CV) systems that also play an important role in quantum information, the standard techniques in use today are decades old, namely homodyne measurement [8, 9] for optical photons and direct Wigner function measurement [10–12] for cavity QED. With the rapid development in CV quantum information processing, ranging from arbitrary state preparation [13] to universal quantum control [14, 15] and from engineered dissipation [16, 17] to quantum error correction [18, 19], a large dimension of Hilbert space can be coherently controlled in experiments [12, 20]. However, homodyne measurement might not be immediately applicable due to intrinsic nonlinearity preventing applying a very large displacement in cavity QED, and Wigner function measurement requires intensive data collection [20]. Thus there is an urgent need for reliable and efficient tomography for CV systems.

There have been significant advances in excitation counting over various physical platforms, including optical photons [21], microwave photons [22–25], and phonons of trapped ions [26–28]. In particular, the capability of quantum non-demolition measurement of microwave excitation number has been demonstrated with

superconducting circuits [29]. Tomography based on excitation counting has also been theoretically proposed [30, 31] and experimentally demonstrated with trapped ions and cavity/circuit QED [25, 26, 32]. However, all these works only considered specific choices of measurement settings (associated with certain displacement patterns), and mostly restricted to the feasibility of tomography, without further investigating the robustness against measurement noise to develop robust QST protocols for CV systems.

Motivated by these recent advances, we develop a theoretical framework to investigate cost-effective QST protocols for CV systems based on excitation counting. Conventional QST protocols can be regarded as special cases collecting *partial* information of the excitation number distribution. For example, up to a displacement, the Husimi Q function can be regarded as the probability of zero excitation, and the Wigner function can be obtained from the difference between probabilities associated with even and odd number of excitations. We expect more cost-effective QST by collecting full population distributions upon various displacements using excitation counting, which can be efficiently achieved in various CV systems [21–29].

The rest of the paper is organized as follows. In Section II, we first provide a mathematical formulation of QST based on displacements and excitation counting. We then consider QST for a special class of quantum states in Section III, illustrating the advantage of excitation counting and introducing the criterion of error robustness in terms of the *condition number* (CN) of the sensing map in Section IV. The main results on QST of a general unknown quantum state are presented in Section V and VI. In Section VII, the choice of optimization target for different error models are analyzed. We put our optimized scheme to the test using simulated measurement records in Section VIII. Section IX discusses possible generalizations of the scheme. Finally, the conclusion is given in

Section X.

II. INFORMATIONAL COMPLETENESS

Mathematically, QST solves the inversion problem

$$A \cdot \vec{\rho} = \vec{b},$$

where $\vec{\rho}$ is the unknown density matrix arranged as a vector, $\vec{b}$ denotes all the measurement records, and A is the sensing matrix determined by the kind of measurements performed. The set of measurements should be *informationally complete* (IC) — that is, the sensing matrix A should be invertible [33]. For non-square sensing matrix, the unknown state can be reconstructed using least squares fitting,

$$\vec{\rho} = \tilde{A}^{-1}\vec{b} = \left(A^{\dagger}A\right)^{-1} A^{\dagger}\vec{b}.$$

Due to experimental noise, the least square solution may turn out non-physical, i.e. having negative eigenvalues. This can be fixed by finding the physical density matrix σ that is closest to ρ, with the distance defined by some matrix norm, e.g. Frobenius norm. A justification of this procedure is provided in Appendix A.

For CV systems, each measurement setting is associated with a displacement operation $D(\beta)$. We may directly count the excitation number after the displacement operation and obtain the number distribution, which is called the *generalized Q function* (Q_n function) [29, 30, 34, 35]

$$Q_n^{\beta}(\rho) = \mathrm{tr}\left[|n\rangle\langle n| D(-\beta)\rho D^{\dagger}(-\beta)\right],$$

where $n = 0, 1, 2, \cdots, n_c$ with n_c the maximal resolved excitation number. Reshaping ρ into a column vector $\vec{\rho}$ we obtain the linear equation $\vec{Q}^{\beta}(\rho) = A^{\beta}\vec{\rho}$, where $\vec{Q}^{\beta}(\rho)$ is a column vector with $(n_c + 1)$ entries $Q_n^{\beta}(\rho)$ and the matrix A^{β} has $(n_c + 1)$ rows. Multiple measurement settings associated with a set of displacements $\left\{\beta_1, \beta_2, \cdots, \beta_{N_\beta}\right\}$ are used to constrain the inversion problem. The measurement record $\vec{b}$ is then a column vector with $N_\beta \cdot (n_c + 1)$ entires of $Q_n^{\beta_j}(\rho)$; the sensing matrix A can be obtained by stacking A^{β_i}, with a total of $N_\beta \cdot (n_c + 1)$ rows. The basis under which ρ is written can be arbitrary, e.g. Fock basis $|m_1\rangle\langle m_2|$ or coherent state basis $|\alpha_i\rangle\langle\alpha_j|$.

In comparison, the sensing matrix for standard QST with the Husimi Q function $Q_{n=0}^{\beta}(\rho) = \langle\beta|\rho|\beta\rangle$ or Wigner function $W^{\beta}(\rho) = \sum_n (-1)^n Q_n^{\beta}(\rho)$ consists of only N_β rows (which are linear combinations of $N_\beta \cdot (n_c + 1)$ rows of the sensing matrix associated with Q_n function [36]), which neglect a large portion of potentially useful information. In the following, we consider QST for a class of quantum states and show that the neglected information can be crucial.

III. QST FOR CAT STATES

Cat states are quantum states characterized by density matrix $\rho = \sum_{i,j=1}^{p} \rho_{ij}|\alpha_i\rangle\langle\alpha_j|$, where $|\alpha_i\rangle$ are well separated coherent states [37]. The Schrödinger cat state $|\alpha\rangle + |-\alpha\rangle$ is a well-known example. Standard QST of cat states with large unknown α's is resource consuming and requires many measurement settings. In particular, both the Husimi and Wigner function measurement schemes encounter the challenge of unknown α's, and have to deploy many measurement settings to scan various displacements, the majority of which is unfortunately wasted because $Q^{\beta}(\rho) \approx W^{\beta}(\rho) \approx 0$ for most choices of β. In contrast, the Q_n function measurement always generates an excitation distribution, from which we can estimate the distances $|\alpha_i - \beta|$ for different β. Using the idea of trilateration, we can estimate all α's using about *three* measurement settings. Using the data $Q_n^{\beta}(\rho)$ for $\{\beta_1, \beta_2, \beta_3\}$, we can estimate the denisty matrix $\tilde{\rho}$ using the iterative maximum likelihood estimation (iMLE) technique [38] and calculate the corresponding Husimi Q function, see Fig. 1 (b). To increase confidence, one can additionally measure $Q_n^{\beta}(\rho)$ at one or two $\beta's$, preferably at the current estimated $\alpha_i's$, see Fig. 1 (c), (d). If the true state is not a cat-state, we would not see clearly separated population patches in the phase space and need to treat it as a general state.

Once the $\alpha's$ are known, the generalized Q function measurement only requires *one additional* measurement setting to fulfill the IC requirement, independent of the number of coherent components. It is note-worthy that examples where tomography requires only one measurement setting is extremely rare. This observation can be justified by the relation

$$\begin{aligned}
Q_n^{\beta}(\rho) &= \sum_{i,j=1}^{p} \rho_{ij} Q_n^{\beta}\left(|\alpha_i\rangle\langle\alpha_j|\right) \\
&= \sum_{i,j=1}^{p} \rho_{ij}\mathrm{tr}\left[|n\rangle\langle n| D(-\beta)|\alpha_i\rangle\langle\alpha_j| D^{\dagger}(-\beta)\right] \\
&= \sum_{i,j=1}^{p} \rho_{ij} e^{i\theta(\beta,\alpha_i,\alpha_j)} e^{-\frac{1}{2}(|\alpha_i-\beta|-|\alpha_j-\beta|)^2} \\
&\quad \times \frac{1}{n!}\left[(\alpha_i-\beta)(\alpha_j-\beta)^*\right]^n e^{-|\alpha_i-\beta|\cdot|\alpha_j-\beta|} \\
&= \sum_{i,j=0}^{p} \tilde{\rho}_{ij}\frac{1}{n!}\left[d_i d_j e^{i\phi_{ij}}\right]^n,
\end{aligned}$$

where we defined

$$\begin{aligned}
d_i &\equiv |\alpha_i - \beta|, \\
\phi_{ij} &\equiv \arg(\alpha_i - \beta) - \arg(\alpha_j - \beta), \\
\theta(\beta, \alpha_i, \alpha_j) &\equiv -i(-\beta\alpha_i^* + \beta^*\alpha_i - \alpha_j\beta^* + \alpha_j^*\beta)/2, \\
\tilde{\rho}_{ij} &\equiv e^{i\theta(\beta,\alpha_i,\alpha_j)} e^{-\frac{1}{2}(d_i-d_j)^2} e^{-d_i d_j}\rho_{ij}.
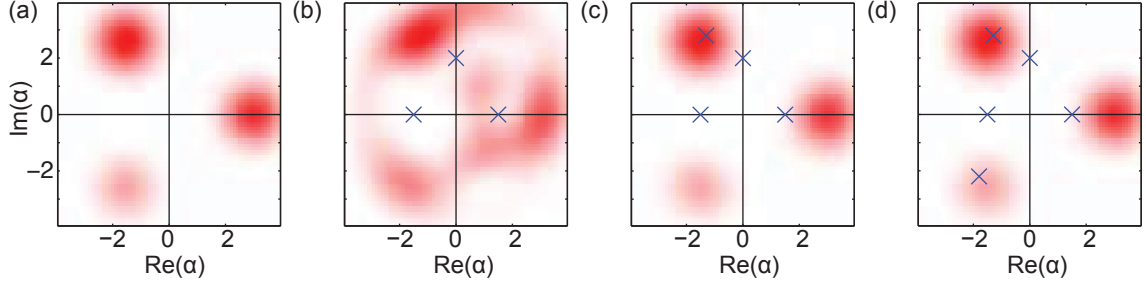\end{aligned}$$

Figure 1. Procedure of estimating the α_i via Husimi Q function. (a) shows the true Q function of the state; (b) shows the estimated Q function via iMLE after measuring $Q_n^\beta(\rho)$ at three $\beta's$ shown as the crosses; (c)/(d) are estimations after measuring at four/five $\beta's$. Apparently estimate in (c) already converges to the true Q function shown in (a).

Reshaping $\tilde{\rho}_{ij}$ as a column vector, we have

$$
\begin{pmatrix}
1 & \cdots & 1 & \cdots \\
\vdots & \ddots & \vdots & \\
d_1^{2n} & \cdots & (d_i d_j e^{i\phi_{ij}})^n & \\
\vdots & & \vdots & \ddots
\end{pmatrix}
\begin{pmatrix}
\tilde{\rho}_{11} \\
\vdots \\
\tilde{\rho}_{ij} \\
\vdots
\end{pmatrix}
=
\begin{pmatrix}
0! Q_0^\beta \\
\vdots \\
n! Q_n^\beta \\
\vdots
\end{pmatrix}.
$$

The matrix on the left hand side is a Vandermonde matrix, having full column rank (all column vectors are independent and $A^\dagger A$ is invertible) if and only if all $d_i d_j e^{i\phi_{ij}}$ are distinct. Under the following conditions, all the $d_i d_j e^{i\phi_{ij}}$ are distinct: (i) $d_i \neq d_j$, other wise the columns corresponding to $\tilde{\rho}_{ii}$ and $\tilde{\rho}_{jj}$ would be identical;; (ii) $\phi_{ij} \neq 0, \pi$, otherwise the columns $\tilde{\rho}_{ij}$ and $\tilde{\rho}_{ji}$ would be identical; (iii) $d_i d_j \neq d_k d_l$ or $\phi_{ij} \neq \phi_{kl}$ where all of i, j, k, l are assumed to be distinct. These requirements have clear geometric interpretations: (i) β does not lie on the perpendicular bisector of the line segment $\alpha_i \alpha_j$; (ii) β, α_i, α_j are not collinear; (iii) triangles formed by $(\beta, \alpha_i, \alpha_j)$ and $(\beta, \alpha_k, \alpha_l)$ do not have the same area or the angles subtended by the segments $\overline{\alpha_i \alpha_j}$ and $\overline{\alpha_k \alpha_l}$ from β are different. There is in fact one extra soft requirement, due to the factor $e^{-\frac{1}{2}(d_i - d_j)^2}$ in $Q_n^\beta(|\alpha_i\rangle\langle\alpha_j|)$. When $d_i \ll d_j$ or $d_i \gg d_j$, ρ_{ij} gets exponentially suppressed and almost vanishes from the sensing equation, just like the case with the conventional Husimi Q function. So we add one requirement (iv) β does not lie far away from the bisector of $\alpha_i \alpha_j$ in the sense that $e^{-\frac{1}{2}(d_i - d_j)^2}$ is not too small. Requirement (iv) is closely related to the error robustness which will be discussed later. The Q_n function at one suitable β contain sufficient information. More specifically, the diagonal terms in the density matrix ρ_{ii} (the population of $|\alpha_i\rangle$) can be extracted from the envelope of the distribution, while the off-diagonal terms $\rho_{i,j}$ can be obtained from the interference signals peaked at $\bar{n} = d_i d_j$ in the distribution. Therefore, sampling the excitation number distribution can boost the information gain and thus reduce the measurement settings significantly.

IV. ERROR ROBUSTNESS OF RECONSTRUCTION

So far, we have only considered the requirement for IC, possibility of reconstruction. We do not yet know the accuracy of the reconstruction when measurements are noisy. Next, we investigate robustness and estimate the reconstruction error. Assume that the measurements $\vec{b}$ have noise $\delta\vec{b}$, leading to noise in the solution $\tilde{A}^{-1}\delta\vec{b}$. To bound the noise in the solution, we consider the worst-case noise magnification ratio

$$
\kappa(A) \equiv \frac{\left\| \tilde{A}^{-1}\delta\vec{b} \right\| / \left\| \tilde{A}^{-1}\vec{b} \right\|}{\left\| \delta\vec{b} \right\| / \left\| \vec{b} \right\|},
$$

which is called the *condition number* (CN) of A [39]. The CN is a property of the sensing map and does not depend on the specific procedure that solves the linear equations. In principle the norm can be chosen arbitrarily. We will use the 2-norm $\|\bullet\|_2$ of vectors, because in this case the CN is simply the ratio of the largest and smallest singular values of A [39]. Clearly $\kappa(A) \geq 1$ and when $\kappa(A) = 1$ the sensing map is isometric (distance preserving). The CN has been introduced as a measure of robustness of reconstruction schemes for qubit systems [40–42]. Using Uhlmann's definition

$$
F(\rho, \sigma) = \mathrm{Tr}\left[\sqrt{\sqrt{\rho}\sigma\sqrt{\rho}} \right],
$$

the reconstruction fidelity can be bounded as (see Appendix B for a proof)

$$
F(\rho, \rho + \delta\rho) \geq 1 - \frac{1}{2}\kappa(A)\sqrt{r}\,\|\rho\|_F \left\| \delta\vec{b} \right\|_2 / \left\| \vec{b} \right\|_2, \quad (1)
$$

where r is the rank of $\delta\rho$ bounded by the system dimension, and $\|\rho\|_F$ is the Frobenius norm of the true density matrix which is fixed. Assuming for now that $\left\| \delta\vec{b} \right\|_2 / \left\| \vec{b} \right\|_2$ is fixed (e.g., due to systematic bias), a robust QST should minimize CN to have an optimal guarantee of the reconstruction fidelity. Note that a lower CN
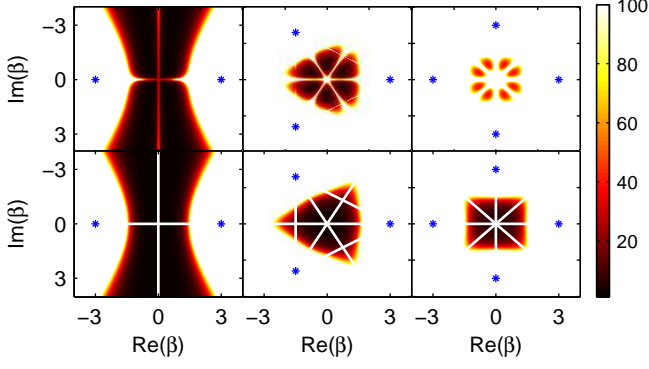
Figure 2. (Color online) Condition number of the sensing map as a function of β for cat states with number of components $p = 2, 3, 4$. **Upper panels:** numerical results for CN; **Lower panels:** a simple estimate of the CN using the expression $\kappa(\beta) \sim \sum_{i,j} \exp\left[(d_i - d_j)^2 / 2\right]$ where $d_i \equiv |\alpha_i - \beta|$. We also included the white lines on which the sensing map is strictly informationally incomplete, see main text. Blue stars indicate the positions of the coherent components $|\alpha_i\rangle$. For visual clarity, values beyond 100 are all mapped to white. The minimum CN achievable for the three cases are 1.74, 6.81 and 38.64 (numerical results), respectively. Here the maximal resolved excitation number n_c is taken sufficiently large. If n_c decreases, CN for large $|\beta|$ gets worse.

reduces the sample complexity but not the computational complexity of the inversion problem.

We now use CN to examine the robustness of QST for cat-states, for which CN is a function of one complex variable β. Due to the factor $e^{-\frac{1}{2}(d_i - d_j)^2}$ in $Q_n^\beta(|\alpha_i\rangle\langle\alpha_j|)$, when $d_i \ll d_j$ or $d_i \gg d_j$, ρ_{ij} gets exponentially suppressed, just like the case with the Husimi Q function. In those regions, the factor $\exp\left[(d_i - d_j)^2 / 2\right]$ would magnify the noise during the reconstruction. Thus we estimate

$$\kappa(\beta) \sim \sum_{i,j} \exp\left[(d_i - d_j)^2 / 2\right],$$

which agrees well with the numerical calculation of CN, as illustrated in Fig. 2. Different from the requirement for IC, CN depends on the number of coherent components p, the values of α_i, and the choice of β. For small p, there exist low-CN regions of β (dark regions in Fig. 2), which imply that the protocol with only about four measurement settings (about three for trilateration and one for coherences) can be robust.

These low-CN regions are very similar to the regions with high Fisher information in the worst case. For the state $\rho = \sum_{i,j=1}^p \rho_{ij} |\alpha_i\rangle\langle\alpha_j|$ with known α_i, the parameters to estimate are ρ_{ij}. For convenience we arrange the p^2 numbers as a vector $\vec{\rho}$. For a certain measurement position β, we can get a distribution

$$f(n) \equiv Q_n^\beta(\vec{\rho}).$$

According to the definition, the Fisher information matrix is

$$\mathcal{I}(\vec{\rho}) = \mathbb{E}_{\vec{\rho}}\left[\left(\frac{\partial}{\partial\vec{\rho}}\log f(n)\right) \cdot \left(\frac{\partial}{\partial\vec{\rho}}\log f(n)\right)^\dagger\right]$$

$$= \sum_{n=0}^\infty \frac{1}{f(n)}\left(\frac{\partial}{\partial\vec{\rho}}f(n)\right) \cdot \left(\frac{\partial}{\partial\vec{\rho}}f(n)\right)^\dagger,$$

where

$$\frac{\partial f}{\partial\rho_{ij}} = Q_n^\beta(|\alpha_i\rangle\langle\alpha_j|).$$

Notice that $\mathcal{I}(\vec{\rho})$ is a matrix-valued function depending on the true state specified by $\vec{\rho}$. We use the determinant of $\mathcal{I}(\vec{\rho})$ as a one-parameter measure of the information contained in the measurement $Q_n^\beta(\rho)$ and plot $\det \mathcal{I}(\vec{\rho})$ as a function of β for a few different $\vec{\rho}$, see Fig. 3.

This justifies the use of CN as a guide for optimizing measurement schemes, which is much easier to calculate than the worst-case Fisher information. For larger p or general states, we need to consider multiple measurement settings and optimized choices of $\beta's$ as discussed below.

V. INFORMATIONAL COMPLETENESS FOR GENERAL STATES

We now consider general states with no structure other than an excitation number cutoff m_c. To achieve IC, we need $N_\beta = (m_c+1)$ different $\beta's$ as argued below. In Fock basis, $\rho = \sum_{m_1,m_2=0}^{m_c} \rho_{m_1,m_2} |m_1\rangle\langle m_2|$, and for each term $|m_1\rangle\langle m_2|$

$$Q_n^\beta(|m_1\rangle\langle m_2|)$$
$$= \frac{|\beta|^{2n}e^{-|\beta|^2}}{n!}\frac{\sqrt{m_1!m_2!}}{(-\beta)^{m_1}(-\beta^*)^{m_2}}\mathcal{L}_{m_1}^{n-m_1}(|\beta|^2)\mathcal{L}_{m_2}^{n-m_2}(|\beta|^2),$$

where $\mathcal{L}_m^n(x)$ is the associated Laguerre polynomial. Note that $\mathcal{L}_m^n(x)$ is not only a polynomial of degree m in x but also a polynomial of degree m in n. Apart from the factor $\frac{|\beta|^{2n}e^{-|\beta|^2}}{n!}$, $Q_n^\beta(|m_1\rangle\langle m_2|)$ is a polynomial of degree $(m_1 + m_2)$ in n. Since $Q_n^\beta(\rho)$ has a degree of $2m_c$ in n, experimental values of of $Q_n^\beta(\rho)$ for each β provides $(2m_c + 1)$ real coefficients,

$$Q_n^\beta(\rho) = \sum_{k=0}^{2m_c} n^k \cdot c_k^\beta.$$

The dependence of c_k^β on $\rho_{m_1 m_2}$ is shown below (omitting β superscript on c_k):
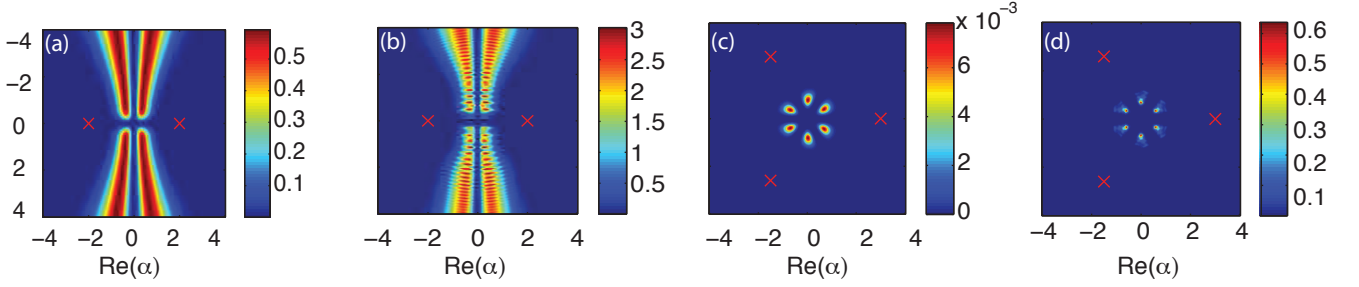
Figure 3. Determinant of the Fisher information $\mathcal{I}(\vec{\rho})$ as a function of β for four different states. (a) Two-component maximally mixed cat state, $\rho_{ij} \propto \delta_{ij}$. In other words, the Bloch vector for the effective two level system is $\vec{0}$; (b) A two component cat state, with Bloch vector $0.9 \cdot (1, 1, 0)/\sqrt{2}$; (c) Three-component maximally mixed cat state, $\rho_{ij} \propto \delta_{ij}$; (d) A mixture $\rho = (1-\lambda)I/3 + \lambda |\psi\rangle \langle\psi|$ where I is the identity and $|\psi\rangle = (1, 1, 1)^{\dagger}\sqrt{3}$. The shape of the good detection region for maximally mixed states are very similar to that predicted by the condition number while for higher purity states additional "interference fringes" appear. The worst case of Fisher information over all true states appears to be that of the maximally mixed states. The good regions for β predicted by worst-case Fisher information agree well with that given by condition number.

$$c_{2m_c} \sim \rho_{m_c, m_c}$$
$$c_{2m_c-1} \sim \rho_{m_c, m_c}, \rho_{m_c-1, m_c}, \rho_{m_c, m_c-1}$$
$$\vdots$$
$$c_{m_c} \sim \rho_{0, m_c}, \rho_{1, m_c-1}, \cdots, \rho_{m_c, 0} \text{ and all above}$$
$$c_{m_c+1} \sim m_c \text{ new terms and all above}$$
$$\vdots$$
$$c_0 \sim \text{all variables above.}$$

For example, knowledge of c_{2m_c} directly reveals ρ_{m_c, m_c} and c_{2m_c-1} gives a linear equation involving ρ_{m_c, m_c-1}, ρ_{m_c-1, m_c} and ρ_{m_c, m_c} which is already obtained from c_{2m_c}. After experimentally obtaining $Q_n^{\beta_1}(\rho)$ and $Q_n^{\beta_2}(\rho)$, the values of ρ_{m_c, m_c-1} and ρ_{m_c-1, m_c} can be determined. Continuing this way we can determine all of ρ_{m_1, m_2} after measuring $Q_n^{\beta}(\rho)$ for (m_c+1) $\beta's$. This analysis is similar to that done in [9].

VI. ERROR ROBUSTNESS FOR GENERAL STATES

It is convenient to consider the covariance matrix,

$$C \equiv A^{\dagger}A = \sum_j A_{\beta_j}^{\dagger} A_{\beta_j},$$

and $\kappa(C) = \kappa(A)^2$. The element $C_{(m_1 m_2),(n_1 n_2)}$ is the overlap of the columns of A corresponding to $|m_1\rangle \langle m_2|$ and $|n_1\rangle \langle n_2|$. In the ideal case, where $\kappa(A) = 1$ and A is an isometry, C should be proportional to the identity

matrix. Using

$$A_{(n,\beta),(m_1,m_2)} = tr\left[D(\beta)|n\rangle\langle n| D(-\beta)|m_1\rangle\langle m_2|\right]$$
$$= e^{-|\beta|^2} \frac{1}{n!} |\beta|^{2n} \frac{\sqrt{m_1!}}{(-\beta)^{m_1}} \mathcal{L}_{m_1}^{n-m_1}\left(|\beta|^2\right)$$
$$\times \frac{\sqrt{m_2!}}{[(-\beta)^{m_2}]^*} \mathcal{L}_{m_2}^{n-m_2}\left(|\beta|^2\right),$$

we see that

$$A_{(n,\beta),(m_1,m_2)} \propto \beta^{m_2-m_1} g_{m_1 m_2}(|\beta|),$$

and

$$C_{(m_1 m_2),(n_1 n_2)} = \sum_{n,j} A_{(n,\beta_j),(m_1,m_2)}^* A_{(n,\beta_j),(n_1,n_2)}$$
$$\propto \sum_{\beta_j} \beta_j^{m_1-m_2-n_1+n_2} f_{m_1,m_2,n_1,n_2}(|\beta_j|),$$

where g and f are real functions that do not have dependence on the complex argument of $\beta's$. Note the convenient fact that the matrix C is additive for parts corresponding to different $\beta's$. Consider a set of $\beta's$ with the same magnitude, $\beta_j = |\beta| e^{i\phi_j}$. Partitioning the indices $(m_1 m_2)$ and $(n_1 n_2)$ into groups according to $k_1 \equiv m_1 - m_2$ and $k_2 \equiv n_1 - n_2$, C has a block structure $C = [C_{k_1 k_2}]$, where elements of the block $C_{k_1 k_2}$ are proportional to $\sum_j e^{-i(k_1-k_2)\phi_j}$.

Both intuitively and rigorously, eliminating the off-diagonal blocks with $k_1 \neq k_2$ would reduce the condition number. This is also known as "pinching" in matrix analysis (see also Appendix C). We may use $N_\beta = (2m_c + 1)$ measurement settings with $\beta's$ evenly distributed over a circle with

$$\phi_j = \frac{2\pi}{2m_c+1}j, \text{ for } j = 0, 1, \cdots, 2m_c,$$

which is denoted as "full-ring configuration" or FRC, as shown in inset of Fig. 7. As pointed out in Appendix C, the multiple-full-ring configuration (MFRC) should

be optimal. However we observed numerically that the improvement of MFRC over the FRC with optimal ring radius is extremely small or even 0. Denote the covariance matrix for a ring of $(2m_c + 1)$ $\beta's$ with radius r as C_r. We compared $\min_r \kappa(C_r)$ and $\min_{r_1, r_2} \kappa(C_{r_1} + C_{r_2})$. For $m_c = 1$ we found a 1.6% difference and for $m_c \geq 2$ (tested up to 7) they are equal. We thus conjecture that FRC is the optimal configuration for $m_c \geq 2$. The number of $\beta's$ required for MFRC is at least twice as large as that of FRC. So practically FRC is much more efficient than MFRC.

Strictly speaking, with a smaller N_β it is not possible to fully pinch matrix C, i.e. satisfying

$$\sum_j e^{-i(k_1 - k_2)\phi_j} \propto \delta_{k_1 k_2},$$

for all k_1, k_2. This justifies the ring based configurations used in [25, 26, 30]. Numerically, however, we find that for large $|\beta|$, the number of measurement settings can be further reduced from $2m_c + 1$ to $m_c + 1$ without compromising CN, as illustrated in Fig. 7. The optimized β's are evenly distributed over half a circle, with

$$\phi_j = \frac{\pi}{m_c + 1} j, \text{ for } j = 0, 1, \cdots, m_c,$$

which is denoted as "half-ring configuration" or HRC, as shown in inset of Fig. 7. For even m_c, the configuration $\phi_j = \frac{2\pi}{m_c+1} j$, for $j = 0, 1, \cdots, m_c$ works as well. The justification of HRC lies in the special asymptotic behavior of matrix C. As $|\beta|$ gets large, the off-diagonal blocks of C_{k_1, k_2} with odd $k_1 - k_2$ scale as $1/|\beta|^2$, negligible compared to those C_{k_1, k_2} with even $k_1 - k_2$ which scales as $1/|\beta|$ (see Appendix F for a proof). So nearly half of those off-diagonal blocks are automatically pinched and we only need to have

$$\sum_j e^{-i(k_1 - k_2)\phi_j} \propto \delta_{k_1 k_2}, \text{ for even } k_1 - k_2,$$

to fully pinch C, which can be achieved using $m_c + 1$ settings. Interestingly, the pinching analysis can be applied to Homodyne detection (see Appendix D) and we verified that the intuitive choice of equally spaced phase angles is optimal. Futhermore, we found that the matrix C for Q_n asymptotes to that of Homodyne detection and so Homodyne detection can in some sense be seen as the Q_n detection with $\beta \to \infty$.

We also performed numerical gradient-based optimization of $\kappa(A)$ over $\beta's$ with different N_β. The gradient of CN with respect to $\beta's$ can be calculated using perturbation theory (detailed in Appendix E). CN drops significantly as N_β increases to $m_c + 1$ and does not improve further when $N_\beta > m_c + 1$. For each N_β we initialize the optimization with a large number of different configurations of $\beta's$ and HRC turns out the best (with the exception of the case $m_c = 1$). As a function of m_c, the asymptotic CN grows slowly, $\kappa(A) \sim m_c^{1/2}$ (see Fig. 5).

VII. DISCUSSION OF NOISE MODELS

So far, we have assumed that $\left\|\delta\vec{b}\right\|_2 / \left\|\vec{b}\right\|_2$ be fixed, and minimize $\kappa(A)$ to optimize the bound in Eq. (1). On the other hand, $\left\|\delta\vec{b}\right\|_2 / \left\|\vec{b}\right\|_2$ might be tunable. A practically relevant situation is shot-noise, with

$$\left\|\delta\vec{b}\right\|_2 / \left\|\vec{b}\right\|_2 \propto 1/\sqrt{N_{rep}}.$$

Meanwhile, $\kappa(A)$ depends on the number of measurement settings N_β. Given total number of measurements (or copies of unknown states) $N_{tot} = N_\beta \cdot N_{rep}$, we need to minimize $\tilde{\epsilon} \equiv \kappa(A) \left\|\delta\vec{b}\right\| / \left\|\vec{b}\right\|$ to have a better bound. Hence,

$$\tilde{\epsilon} \propto \kappa(A)/\sqrt{N_{rep}} = \kappa(A)\sqrt{N_\beta/N_{tot}}$$

implies that we should minimize $\kappa(A)\sqrt{N_\beta}$. As illustrated in the bottom inset of Fig. 7, HRC has lower $\kappa(A)\sqrt{N_\beta}$ for large $|\beta|$, and is more robust than FRC in that regime. In terms of scaling with m_c,

$$\kappa(A)\sqrt{N_\beta} \sim m_c^{1/2}\sqrt{m_c + 1} \sim m_c$$

for HRC and FRC while $\kappa(A)\sqrt{N_\beta}$ appears super-linear in m_c for Wigner tomography, as shown in Fig. 6. The relative advantage of Q_n tomography grows as m_c increases.

VIII. BENCHMARKING WITH SIMULATED DATA

Using simulated data (shot-noise only), we tested and compared several schemes, including Wigner measurements where $\beta's$ form a square lattice (yellow triangles), Wigner measurements with optimized $\beta's$ (red squares), and Q_n measurements with optimized $\beta's$ (blue circles). For each case reconstruction is done by fitting a physical density matrix to the data, a semidefinite program that can be solved efficiently with the Matlab package CVX [43, 44]. Some typical results with $m_c = 2$ and $m_c = 5$ are shown in Fig. 4. Both optimized schemes have better error scaling than the unoptimized one, because the bound for the unoptimized case is too forgiving to suppress reconstruction error. Between the two optimized schemes, the reconstruction infidelity for the Q_n-based scheme is at least an order of magnitude smaller than that of the Wigner-based scheme. Moreover, the advantage of using Q_n measurement and more generally optimized schemes indeed becomes more significant for larger m_c, as predicted by the figure of merit shown in Fig. 6 and demonstrated by Fig. 4.
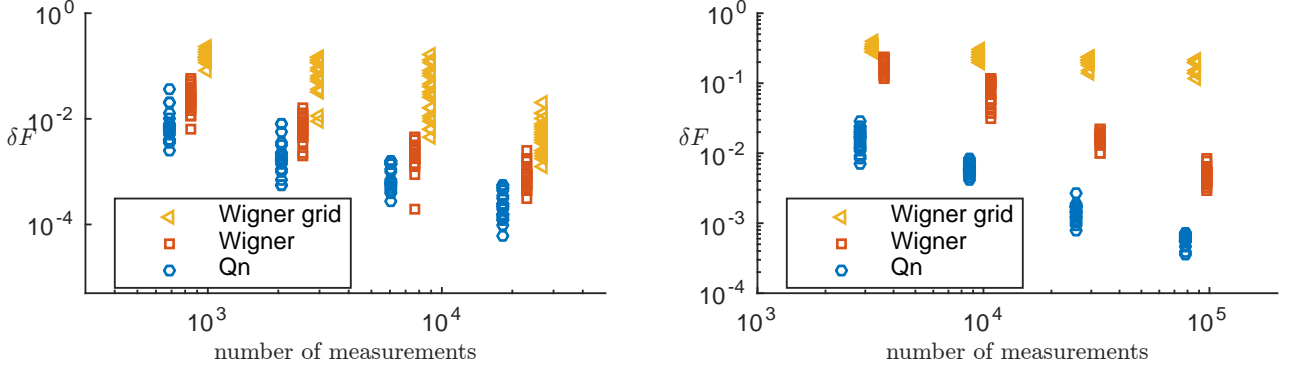
Figure 4. (Color online) Comparison of performances of Wigner measurements where $\beta's$ form a square lattice (yellow triangles), Wigner measurements with optimized measurement settings obtained from gradient search (red squares), and Q_n measurements with optimized measurement settings (blue circles). **Left/Right panels** correspond to $m_c = 2$ and $m_c = 5$. The true state ρ is a randomly generated density matrix with excitation number cutoff $m_c = 5$. Each scatter point corresponds to one reconstruction via semi-definite programming based on a set of simulated measurement records containing only shot-noise. The y-axis shows the reconstruction infidelity $\delta F = 1 - F(\rho, \rho')$ and the x-axis shows the total number of measurements performed, i.e. total number of copies of unknown states consumed.
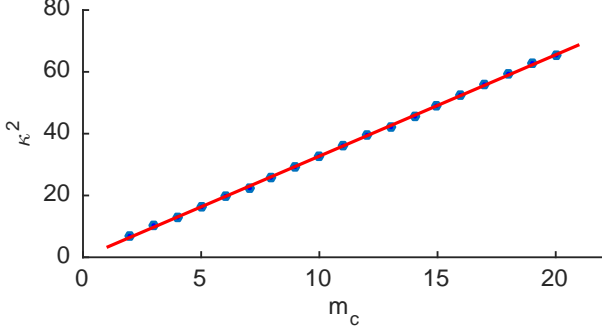

Figure 5. Optimal condition number for Q_n measurements as a function of m_c. Vertical axis shows $\kappa(A)^2$. Red solid line shows a linear fit with equation $\kappa^2 = 3.28 m_c - 0.07769$.
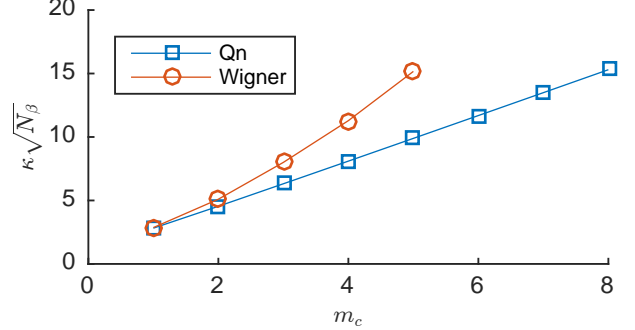

Figure 6. Comparison of the figures of merits (assuming shot-noise only) $\kappa\sqrt{N_\beta}$ for optimized Q_n tomography with large enough $|\beta|$ and optimized Wigner tomography obtained from gradient-based optimization.

IX. GENERALIZATIONS

The idea of optimizing the condition number of the measurement scheme is completely general and can apply to the reconstruction problem using arbitrary bases. Here we show one such example, the generalized cat states,

$$\rho = \sum_{i,j,m_1,m_2} \rho_{i,m_1;j,m_2} |\alpha_i, m_1\rangle \langle \alpha_j, m_2|,$$

where $i, j = 1, 2, \cdots, p$ and $m_1, m_2 = 0, 1, \cdots, m_c$, and

$$|\alpha_i, m_i\rangle \equiv D(\alpha_i) |m_i\rangle$$

are displaced Fock states. Such states may arise when an ideal cat state is subject to experimental noise and each coherent state component is deformed. Now each column of the sensing matrix has the form

$$(d_i d_j e^{i\phi_{ij}})^n P(n),$$

where $P(n)$ is a polynomial coming from the associated Laguerre polynomials

$$P(n) = \mathcal{L}_{m_1}^{n-m_1}(|\beta|^2)\mathcal{L}_{m_2}^{n-m_2}(|\beta|^2).$$

On a large scale of n, the change of $(d_i d_j e^{i\phi_{ij}})^n P(n)$ as a function of n is dominated by the exponential part $(d_i d_j e^{i\phi_{ij}})^n$. So just as in the cat state case the columns with distinct $d_i d_j e^{i\phi_{ij}}$ are linearly independent. For the $(m_c + 1)^2$ columns that share the same $d_i d_j e^{i\phi_{ij}}$ but different polynomials $P(n)$, we need (m_c+1) different β's to completely fix all unknowns as discussed previously. We can then run numerical optimization for all $N \geq (m_c+1)$ and pick the optimal N.

A simultaneous optimization of many $\beta's$ can often get stuck in shallow local minima. Here we show an alternative greedy-policy for optimization that works pretty well, where we pick one best β at a time. The procedure is as follows. (1) Start with an empty set $S = \emptyset$ of
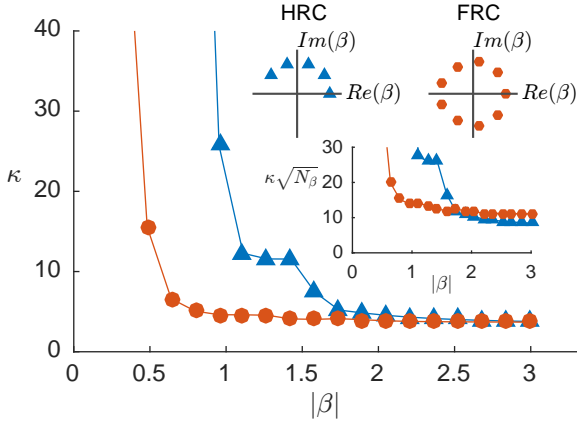
Figure 7. (Color online) **Main panel** shows condition numbers of full-ring configuration (FRC) and half-ring configuration (HRC) as a function of the ring radius ($m_c = 4$ case). **Top two insets** show FRC and HRC in phase space. For both schemes, $\beta_j = |\beta| e^{i\phi_j}$. FRC: $\phi_j = \frac{2\pi}{2m_c+1} j$, $j = 0, 1, 2, \cdots, 2m_c$; HRC: $\phi_j = \frac{\pi}{2m_c+1} j$, $j = 0, 1, 2, \cdots, m_c$. The condition number of HRC approaches that of FRC as $|\beta|$ gets large, as predicted by theory. **Bottom inset** shows the figure of merit $\kappa \sqrt{N_\beta}$ for HRC and FRC.

$\beta's$, keeping all the $\alpha's$ but set $m_c = 0$, which allows the condition number to be finite with one β; (2) Pick the optimal β (in the sense that it combined with those $\beta's$ in S produces the lowest condition number) and add it to the set S; (3) If the optimal condition number is small enough, increase m_c by one (otherwise keep it the same); (4) Repeat (2) and (3) until one reaches the desired m_c.

We give one example here for which the condition number as a function of the next β to pick are shown in Fig. 8.

X. CONCLUSION

We proposed and analyzed a continuous variable QST scheme with the full distribution information of excitation number after a variable displacement. We showed how to construct a set of measurements that has a small reconstruction error bound by optimizing a figure of merit based on the condition number of the sensing map. For general states with a given excitation number cutoff, we obtained the optimal displacement patterns (half-ring and full-ring) that rationalize and improve the previously considered ring-based choices. The idea of gradient-based optimization of the condition number of the sensing map is versatile and can apply to states expanded in an arbitrary basis and detection methods that are parameterized by some continuous variables. As future work, it is interesting to generalize the current scheme to QST for multiple oscillators, spin ensembles [45] and CV process tomography.

Appendix A: Reconstructing A Physical Density Matrix

Let $\vec{\rho'}$ be the least square solution (potentially non-physical) from the noisy measurement record,

$$\vec{\rho'} = \left(A^\dagger A\right)^{-1} A^\dagger \left(\vec{b} + \delta\vec{b}\right).$$

We claim that the physical density matrix τ that is closest to ρ' in the sense of some norm (say, Frobenius norm) can only be a better estimate of the true state ρ, i.e.

$$\|\tau - \rho\|_F \leq \|\rho' - \rho\|_F. \tag{A1}$$

We now prove the above equation by contradiction. Suppose $\|\tau - \rho\|_F > \|\rho' - \rho\|_F$. Now consider the triangle whose vertices are ρ, ρ' and τ. Let $\theta \in [0, \pi]$ be the angle at the vertex τ. Using the Law of Cosines, we have that

$$\cos\theta = \frac{\|\rho' - \tau\|_F^2 - \|\rho - \rho'\|_F^2 + \|\rho - \tau\|_F^2}{2 \|\rho' - \tau\|_F \|\rho - \tau\|_F} > 0.$$

This implies that $0 \leq \theta < \pi/2$, i.e., the angle at τ is less than 90 degrees.

Hence, there exists a point ζ that is a convex combination of τ and ρ such that

$$\|\zeta - \rho'\|_F < \|\tau - \rho'\|_F.$$

Moreover, since ρ and τ are physical density matrices and the space of density matrices is convex, it follows that ζ is also physical. This contradicts the assumption that "τ is the physical density matrix τ that is closest to ρ'". Therefore, we conclude that Eq. (A1) must hold.
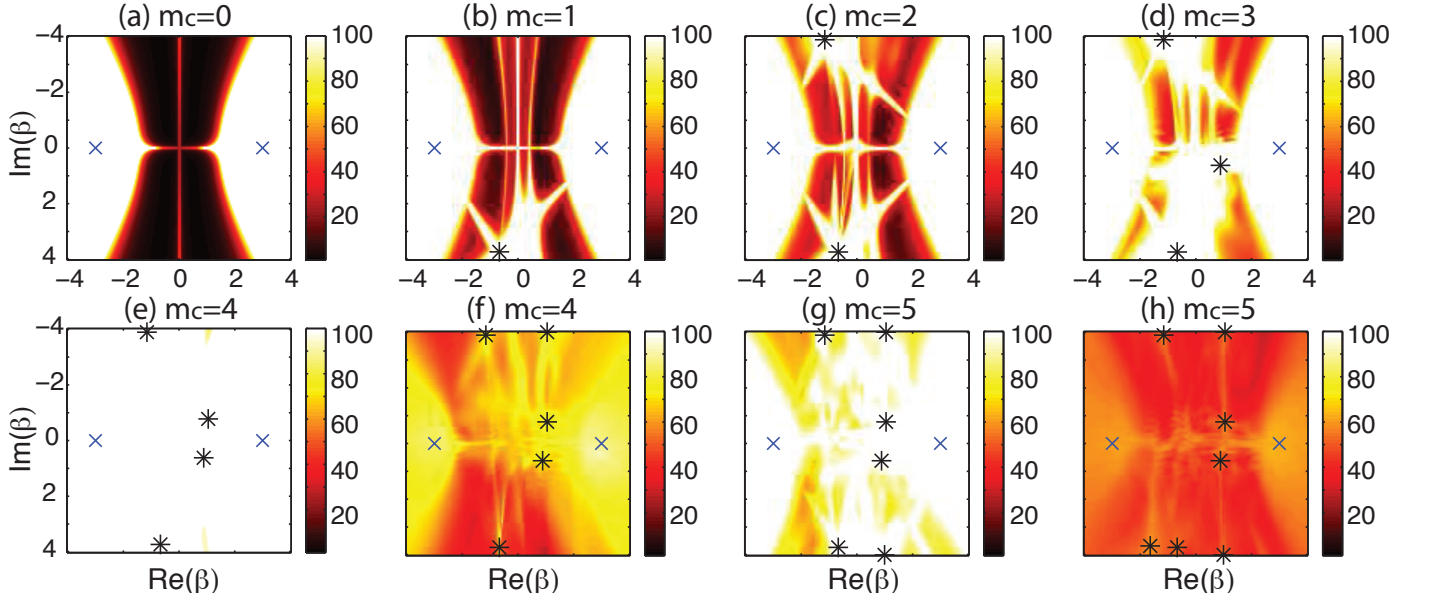
Figure 8. Greedy optimization of the set of $\beta's$. Crosses show the position of $\alpha's$ and stars indicate all the $\beta's$ added to the set S. At each step, the optimal β is added to the set S. When the condition number is low enough (smaller than a preset threshold), m_c is increased by one and the optimization goes on.

Practically, τ can be obtained as the solution of the following semidefinite program (SDP),

$$\text{minimize } \|\sigma - \rho'\|_F$$
$$\text{subject to } \sigma \succeq 0, \ \text{tr}\sigma = 1.$$

Note that SDP can be solved efficiently using the Matlab package CVX [43, 44].

Alternatively, a physical reconstruction τ' may be obtained by directly solving the least square problem in the space of physical density matrices, i.e.

$$\text{minimize } \left\|A \cdot \vec{\sigma} - \vec{b}'\right\|_2$$
$$\text{subject to } \sigma \succeq 0, \ \text{tr}\sigma = 1.$$

Appendix B: Bound for Reconstruction Error

We derive lower bound on the fidelity of reconstruction in terms of condition number here. We will first find a upper bound for the trace distance of the reconstructed state to the true state, and then get the fidelity bound using the relation between fidelity and trace distance $D(\rho, \sigma)$,

$$F(\rho, \sigma) \geq 1 - D(\rho, \sigma)$$

where $D(\rho, \sigma) = \frac{1}{2}\|\rho - \sigma\|_{\text{tr}}$.

Let $\vec{\rho}$ be the true state and $\vec{\rho'}$ be the least square solution from the noisy measurement record,

$$\vec{\rho} = \left(A^\dagger A\right)^{-1} A^\dagger \vec{b},$$
$$\vec{\rho'} = \left(A^\dagger A\right)^{-1} A^\dagger \left(\vec{b} + \delta\vec{b}\right),$$

and define $\delta\vec{\rho} \equiv \vec{\rho} - \vec{\rho'} = \tilde{A}^{-1}\delta\vec{b} = \left(A^\dagger A\right)^{-1} A^\dagger \delta\vec{b}$.

Following the main text we use the 2-norm for vectors $\vec{\rho}$ to define the condition number, then

$$\left(\frac{\|\delta\vec{\rho}\|_2}{\|\vec{\rho}\|_2}\right) \Big/ \left(\frac{\|\delta\vec{b}\|_2}{\|\vec{b}\|_2}\right) \leq \kappa(A).$$

Since the Frobenius norm of a matrix is the same as the 2-norm of it when arranged as a vector,

$$\|\rho\|_F = \|\vec{\rho}\|_2 \leq \kappa(A) \|\rho\|_F \frac{\left\|\delta\vec{b}\right\|_2}{\left\|\vec{b}\right\|_2}.$$

Let τ be physical density matrix that best satisfies the noisy measurement record $A\tau = \vec{b} + \delta\vec{b}$, obtained as described in the previous section. We have

$$\|\rho - \tau\|_{\mathrm{F}} \leq \|\rho - \rho'\|_{\mathrm{F}} = \|\delta\rho\|_F \leq \kappa(A) \|\rho\|_F \frac{\left\|\delta\vec{b}\right\|_2}{\left\|\vec{b}\right\|_2},$$

where the first inequality uses Eq. (A1). The above bound is useful since it upper bounds the distance (in terms of Frobenius norm) between the reconstructed state and the true state.

Using the relation between the trace norm and Frobenius norm

$$\|M\|_{\mathrm{tr}} \leq \sqrt{r} \|M\|_F,$$

we find

$$D(\rho, \tau) \leq \frac{1}{2}\sqrt{r} \|\rho - \tau\|_{\mathrm{F}} \leq \frac{1}{2}\sqrt{r}\kappa(A) \|\rho\|_F \frac{\left\|\delta\vec{b}\right\|_2}{\left\|\vec{b}\right\|_2}$$

and

$$F(\rho, \tau) \geq 1 - D(\rho, \tau) \geq 1 - \frac{1}{2}\sqrt{r}\kappa(A) \|\rho\|_F \frac{\left\|\delta\vec{b}\right\|_2}{\left\|\vec{b}\right\|_2}. \tag{B1}$$

In practice we have an estimate for the measurement noise $\epsilon \sim \frac{\left\|\delta\vec{b}\right\|_2}{\left\|\vec{b}\right\|_2}$ and the truncation dimension d upperbounds the rank r of $\delta\rho$. Since ρ is unknown we replace it with the reconstructed τ. In this way an approximate bound on the fidelity can be calculated, $F(\rho, \tau) \gtrsim 1 - \frac{1}{2}\epsilon\sqrt{d}\kappa(A) \|\tau\|_F$.

Appendix C: Discussion of Full/Half Ring Configurations

The Pinching Inequality

Mathematically, wiping out all the off-diagonal blocks is called "pinching" and is formally described as

$$C \mapsto \tilde{C} = \sum_k P_k C P_k,$$

where P_k is the projector to the subspace corresponding to the block C_{kk}. It is known that the eigenvalues of $\tilde{C}$ are majorized by those of C (see page 50 of [39]), i.e. $\sum_{i=1}^{k} \lambda_i^{\downarrow}(\tilde{C}) \leq \sum_{i=1}^{k} \lambda_i^{\downarrow}(C)$ for $k = 1, 2, \cdots, D$ and $\sum_{i=1}^{D} \lambda_i^{\downarrow}(\tilde{C}) = \sum_{i=1}^{D} \lambda_i^{\downarrow}(C)$, where $\lambda_i^{\downarrow}$ are the eigenvalues in descending order and D is the dimension of C and $\tilde{C}$. This implies that $\kappa(\tilde{C}) \leq \kappa(C)$. This fact can also be understood in the language of quantum mechanics. View $\tilde{C}$ as a block-diagonal Hamiltonian H_0 and $C - \tilde{C}$ as a perturbation H_1 coupling different subspaces of H_0. It is well known that energy levels repel each other when coupled to each other. So the highest of energy level gets higher and the lowest gets lower, with their ratio being increased.

This means that among the sets of $\beta's$ with the same magnitude, the full-ring configuration (FRC) can give the optimal condition number (CN).

Multiple full-ring configuration gives lowest condition number

We now argue that the multiple full-ring configuration (MFRC) can give the minimal condition number if we do not limit the number of measurement settings. Here is our two-step argument. (a) Given a candidate configuration $\{\beta_i\}$ distributed on a ring, i.e. $|\beta_i| = r$, we can always decrease CN by rearranging/adding $\beta's$ such that the configuration becomes FRC, i.e. pinching the covariance matrix. (b) For any given candidate set $\{\beta_i\}$ distributed on different rings, we can always decrease the condition number by rearranging/adding $\beta's$ such that the configuration becomes a collection of FRC (MFRC) to pinch the covariance matrix.

Numerically we observed that usually one full-ring is as good as the multiple full-ring configuration, except the case with $m_c = 1$ where a 1.6% difference between single-ring and double-ring configurations is found.

Half-ring configuration approximates full-ring well

We find it possible to simplify FRC further. With less than $(2m_c + 1)$ points, it is impossible to exactly satisfy $\sum_j e^{i(k_1 - k_2)\phi_j} = \delta_{k_1 k_2}$ for all k_1, k_2. However, we find a very special asymptotic behavior of the covariance matrix, as stated by the following theorem (see Appendix F for the proof).

Theorem 1. *The large-$|\beta|$ asymptotic form of $C_{m_1 m_2, m_3 m_4}(\beta)$ is*

$$C_{m_1 m_2, m_3 m_4}(\beta) \sim \begin{cases} g(m_1,\, m_2,\, m_3,\, m_4,\, \phi)/|\beta|, & \sum_{i=1}^{4} m_i \text{ is even;} \\ g(m_1,\, m_2,\, m_3,\, m_4,\, \phi)/|\beta|^2, & \sum_{i=1}^{4} m_i \text{ is odd;} \end{cases}$$

where ϕ is the complex angle of β.

This theorem effectively says that the elements of $C(\beta)$ has a **"parity selection rule"**.

So in the large $|\beta|$ limit, the block $C_{k_1 k_2} \sim 1/|\beta|$ if $k_1 - k_2$ is even and $C_{k_1 k_2} \sim 1/|\beta|^2$ if $k_1 - k_2$ is odd. Certainly, all diagonal blocks $C_{kk} \sim 1/|\beta|$. So if $|\beta|$ is large enough, the blocks with odd $(k_1 - k_2)$ automatically vanish. To make the rest of the off-diagonal blocks vanish, we only need to choose a configuration such that $\sum_j e^{i(k_1 - k_2)\phi_j} = \delta_{k_1 k_2}$ holds for even $k_1 - k_2 = 2l$, where $l = 0,\, \pm 1,\, \pm 2,\, \cdots,\, \pm m_c$, i.e.

$$\sum_j e^{2il\phi_j} = \delta_{l,0}.$$

It is straightforward to check that the half-ring configuration (HRC), $\phi_j = \frac{\pi}{m_c+1} j$ qualifies for all m_c and $\phi_j = \frac{2\pi}{m_c+1} j$ qualifies for even m_c. In fact for even m_c, $\phi_j = \frac{2\pi n}{m_c+1} j$ could work for any non-zero integer n. Therefore if the optimal radius of FRC is large (which as we will show is usually the case), HRC should work equally well with only half of the measurements.

Appendix D: Optimal Setting For Homodyne Measurement

The pinching analysis to Homodyne tomography follows the Q_n case closely. The term $|m_1\rangle \langle m_2|$ contributes the Homodyne signal

$$\mathcal{H}(|m_1\rangle \langle m_2|) = \text{tr}\left[|x_\theta\rangle \langle x_\theta| \cdot |m_1\rangle \langle m_2|\right]$$
$$= \frac{e^{i(m_1 - m_2)\theta}}{\pi^{1/2}\sqrt{2^{m_1+m_2} m_1! m_2!}} e^{-x^2} H_{m_1}(x) H_{m_2}(x).$$

And the covariance matrix is

$$C_{m_1 m_2, m_3 m_4} = \frac{e^{i(m_3 - m_4 - m_1 + m_2)\theta}}{\pi \sqrt{2^{m_1+m_2+m_3+m_4} m_1! m_2! m_3! m_4!}} \int_{-\infty}^{+\infty} e^{-2x^2} H_{m_1}(x) H_{m_2}(x) H_{m_3}(x) H_{m_4}(x)$$
$$\equiv \frac{e^{i(m_3 - m_4 - m_1 + m_2)\theta}}{\pi \sqrt{2^{m_1+m_2+m_3+m_4} m_1! m_2! m_3! m_4!}} g(m_1, m_2, m_3, m_4).$$

Due to the properties of the Hermite polynomials (i.e. $H_n(x)$ is a odd/even function of x if n is odd/even), if $m_1 + m_2 + m_3 + m_4$ is odd, the integral

$$\int_{-\infty}^{+\infty} dx\, e^{-2x^2} H_{m_1}(x) H_{m_2}(x) H_{m_3}(x) H_{m_4}(x) = 0.$$

To pinch the covariance matrix, we can use the half-ring configuration, i.e. pick $(m_c + 1)$ θ_j such that $\theta_j = \frac{\pi}{2m_c+1} j$ where $j = 0, 1, 2, \cdots, m_c$.

Plugging definite values for m_1, m_2, m_3, m_4, we find the covariance matrix for Homodyne to be the same (up to global a constant) as the asymptotic covariance matrix for Q_n measurements.

Appendix E: Numerical Calculation of the Gradient of the Condition Number

We briefly outline how to calculate the gradient of a matrix's condition number using perturbation theory, in the context of the state tomography problem.

Let us perturbe matrix A by changing β_i infinitesimally,

$$A(\beta_i + \delta\beta_i) = A + \delta\beta_i(\partial_{\beta_i} A)$$
$$\equiv A + \delta\beta_i B_i,$$

where matrix B_i can be calculated from the explicit expression of A. Note that we are changing only one β_i so there's no summation over i here. We try to find $\partial_{\beta_i}\kappa(A)$. For convenience we choose to work with the Hermitian covariance matrix $C \equiv A^\dagger A$ whose condition number is $\kappa(C) = \kappa(A^\dagger A) = \kappa(A)^2$.

$$\partial_{\beta_i}\kappa(C) = \partial_{\beta_i}\frac{\epsilon_{\max}(C)}{\epsilon_{\min}(C)}$$
$$= \frac{\partial_{\beta_i}\epsilon_{\max}(C)\epsilon_{\min}(C) - \epsilon_{\max}(C)\partial_{\beta_i}\epsilon_{\min}(C)}{\epsilon_{\min}(C)^2}, \tag{E1}$$

where $\epsilon_{\max}/\epsilon_{\min}$ are the largest/smallest eigenvalues of C. Now the problem reduces to calculate the gradient of the eigenvalues of C with respect to β_i.

It is well known in quantum mechanics that the first order perturbation to the energy of the k-th eigenstate is

$$\delta\epsilon_k = \langle\psi_k|\,\delta H\,|\psi_k\rangle$$

where $|\psi_k\rangle$ is the k-th eigenstate of the unperturbed Hamiltonian H and δH is a small perturbation.

In our case,

$$C(\beta_i + \delta\beta_i) = C + \delta\beta_i(B_i^\dagger A + A^\dagger B_i) + O(\delta\beta^2),$$

so

$$\partial_{\beta_i}\epsilon_{\mathrm{k}}(C) = v_k^\dagger(B_i^\dagger A + A^\dagger B_i)v_k, \tag{E2}$$

where v_k is the k-th eigenvector of C.

Appendix F: Proof of Theorem 1

For completeness, we provide the detailed proof of theorem 1 in this appendix.

Theorem. *The large-$|\beta|$ asymptotic form of $C_{m_1m_2,m_3m_4}(\beta)$ is*

$$C_{m_1m_2,m_3m_4}(\beta) \sim \begin{cases} g(m_1,\, m_2,\, m_3,\, m_4,\, \phi)/|\beta|, & \sum_{i=1}^{4} m_i \text{ is even;} \\ g(m_1,\, m_2,\, m_3,\, m_4,\, \phi)/|\beta|^2, & \sum_{i=1}^{4} m_i \text{ is odd;} \end{cases}$$

where ϕ is the complex angle of β.

<div align="center">**Some Preparation**</div>

Lemma 2. *Let $I_\nu(z)$ denote the modified Bessel functions of the first kind. For any non-negative integer k, we have*

$$\frac{\partial^k}{\partial z^k}\left[(2\sqrt{z})^\nu I_\nu(2\sqrt{z})\right] = 2^k\left[(2\sqrt{z})^{\nu-k}I_{\nu-k}(2\sqrt{z})\right],$$

$$\frac{\partial^k}{\partial z^k}\left[(2\sqrt{z})^{-\nu} I_\nu(2\sqrt{z})\right] = 2^k\left[(2\sqrt{z})^{-(\nu+k)}I_{\nu+k}(2\sqrt{z})\right],$$

Proof. These can be verified using the properties of $I_\nu(z)$. $\qquad\square$

Lemma 3. *Let n, j_1, j_2, j_3, j_4 be non-negative integers, we have*

$$\sum_{n=0}^\infty \frac{z^n}{(n!)^2}\binom{n}{j_1}\binom{n}{j_2}\binom{n}{j_3}\binom{n}{j_4}$$

$$= \frac{1}{j_1!j_2!j_3!j_4!}z^{j_4}\frac{\partial^{j_4}}{\partial z^{j_4}}z^{j_3}\frac{\partial^{j_3}}{\partial z^{j_3}}z^{j_2}\frac{\partial^{j_2}}{\partial z^{j_2}}z^{j_1}\frac{\partial^{j_1}}{\partial z^{j_1}}I_0(2\sqrt{z})$$

$$= \sum_{k_4=0}^{j_4}\sum_{k_3=0}^{j_3}\frac{j_4!}{k_4!(j_4-k_4)!}\frac{j_3!}{k_3!(j_3-k_3)!}\frac{j_2!}{(j_2-k_3)!}\frac{(j_2+j_3-k_3)!}{(j_2+j_3-k_3-k_4)!}(\sqrt{z})^{j_1+j_2+j_3+j_4-k_3-k_4}I_{j_1-j_2-j_3-j_4+k_3+k_4}(2\sqrt{z}).$$

where $I_0(2\sqrt{z}) = \sum_{n=0}^\infty \frac{z^n}{(n!)^2}$.

Proof. It is straightforward to show tha

$$\sum_n \frac{z^n}{(n!)^2}\binom{n}{j} = \frac{1}{j!}\sum_n \frac{z^n}{(n!)^2}n(n-1)\cdots(n-j+1) = \frac{1}{j!}z^j\frac{\partial^j}{\partial z^j}I_0(2\sqrt{z}).$$

Similarly,

$$\sum_{n=0}^\infty \frac{z^n}{(n!)^2}\binom{n}{j_1}\binom{n}{j_2}\binom{n}{j_3}\binom{n}{j_4} = \frac{1}{j_1!j_2!j_3!j_4!}z^{j_4}\frac{\partial^{j_4}}{\partial z^{j_4}}z^{j_3}\frac{\partial^{j_3}}{\partial z^{j_3}}z^{j_2}\frac{\partial^{j_2}}{\partial z^{j_2}}z^{j_1}\frac{\partial^{j_1}}{\partial z^{j_1}}I_0(2\sqrt{z}).$$

We now try to express the above quantity in an explicit form.

First, using Lemma 2,

$$\frac{\partial^{j_1}}{\partial z^{j_1}}I_0(2\sqrt{z}) = 2^{j_1}\left[(2\sqrt{z})^{-j_1}I_{-j_1}(2\sqrt{z})\right].$$

Next,

$$\frac{\partial^{j_2}}{\partial z^{j_2}}z^{j_1}\frac{\partial^{j_1}}{\partial z^{j_1}}I_0(2\sqrt{z}) = 2^{j_2-j_1}\left[(2\sqrt{z})^{j_1-j_2}I_{j_1-j_2}(2\sqrt{z})\right].$$

Continuing this, we can get

$$\frac{\partial^{j_3}}{\partial z^{j_3}}z^{j_2}\frac{\partial^{j_2}}{\partial z^{j_2}}z^{j_1}\frac{\partial^{j_1}}{\partial z^{j_1}}I_0(2\sqrt{z}) = 2^{j_2-j_1}\frac{\partial^{j_3}}{\partial z^{j_3}}z^{j_2}\left[(2\sqrt{z})^{j_1-j_2}I_{j_1-j_2}(2\sqrt{z})\right]$$

$$= 2^{j_2-j_1}\sum_{k_3=0}^{j_3}\binom{j_3}{k_3}\frac{\partial^{k_3}}{\partial z^{k_3}}(z^{j_2})\frac{\partial^{j_3-k_3}}{\partial z^{j_3-k_3}}\left[(2\sqrt{z})^{j_1-j_2}I_{j_1-j_2}(2\sqrt{z})\right]$$

$$= 2^{j_3+j_2-j_1}\sum_{k_3=0}^{j_3}\binom{j_3}{k_3}\frac{\partial^{k_3}}{\partial z^{k_3}}(z^{j_2})2^{-k_3}\left[(2\sqrt{z})^{j_1-j_2-j_3+k_3}I_{j_1-j_2-j_3+k_3}(2\sqrt{z})\right]$$

Eventually we obtain

$$z^{j_4}\frac{\partial^{j_4}}{\partial z^{j_4}}z^{j_3}\frac{\partial^{j_3}}{\partial z^{j_3}}z^{j_2}\frac{\partial^{j_2}}{\partial z^{j_2}}z^{j_1}\frac{\partial^{j_1}}{\partial z^{j_1}}I_0(2\sqrt{z})$$

$$= \sum_{k_4=0}^{j_4}\sum_{k_3=0}^{j_3}\frac{j_4!}{k_4!(j_4-k_4)!}\frac{j_3!}{k_3!(j_3-k_3)!}\frac{j_2!}{(j_2-k_3)!}\frac{(j_2+j_3-k_3)!}{(j_2+j_3-k_3-k_4)!}(\sqrt{z})^{j_1+j_2+j_3+j_4-k_3-k_4}I_{j_1-j_2-j_3-j_4+k_3+k_4}(2\sqrt{z}).$$

Note that in the above derivation, factors like

$$\frac{a!}{(a-b)!} = a(a-1)(a-2)\cdots(a-b+1)$$

are naturally interpreted as 0 if $a < b$. □

Lemma 4. *Let m be a positive integer and k is a non-negative integer,*

$$\sum_{i=0}^{m}(-1)^i \binom{m}{i} i^k = \begin{cases} 0, & \text{if } 0 \le k < m; \\ (-1)^m m!, & \text{if } k = m; \\ (-1)^m m! \binom{m+1}{2}, & \text{if } k = m+1. \end{cases}$$

Proof. Let α be any real number,

$$(1+\alpha)^m = \sum_{i=0}^{m}\alpha^i \binom{m}{i}.$$

We then have

$$(\alpha\frac{\partial}{\partial\alpha})^k(1+\alpha)^m = \sum_{i=0}^{m} i^k\alpha^i \binom{m}{i}.$$

Defining $x \equiv 1 + \alpha$, we have

$$\alpha\frac{\partial}{\partial\alpha} = (\alpha+1-1)\frac{\partial}{\partial(\alpha+1)} = (x-1)\frac{\partial}{\partial x} = x\frac{\partial}{\partial x} - \frac{\partial}{\partial x}.$$

So

$$\sum_{i=0}^{m}(-1)^i \binom{m}{i} i^k = (\alpha\frac{\partial}{\partial\alpha})^k(1+\alpha)^m\bigg|_{\alpha=-1}$$

$$= \left(x\frac{\partial}{\partial x} - \frac{\partial}{\partial x}\right)^k x^m\bigg|_{x=0}. \tag{F1}$$

Expanding $\left(x\frac{\partial}{\partial x} - \frac{\partial}{\partial x}\right)^k$ we will get 2^k terms, among which those that contain l factors of $-\frac{\partial}{\partial x}$ would reduce the power of x^m by l (note that the factor $x\frac{\partial}{\partial x}$ preserves the power of x). The only term surviving in Eq. (F1) is x^0. Clearly when $k < m$, all the terms have power at least $m - k$. When $k = m$, the only term surviving is

$$\left(-\frac{\partial}{\partial x}\right)^m x^m = (-1)^m m!.$$

For $k = m+1$, there are $m+1$ surviving term each of which has m factors of $-\frac{\partial}{\partial x}$ and one factor of $x\frac{\partial}{\partial x}$. They differ by the position where $x\frac{\partial}{\partial x}$ appear. Consider the term with the i-th factor being $x\frac{\partial}{\partial x}$, it is

$$\left(-\frac{\partial}{\partial x}\right)^{i-1} x\frac{\partial}{\partial x}\left(-\frac{\partial}{\partial x}\right)^{m+1-i} x^m = (-1)^m \left(\frac{\partial}{\partial x}\right)^{i-1} x\frac{\partial}{\partial x}\frac{m!}{(i-1)!}x^{i-1}$$

$$= (-1)^m(i-1)!\frac{m!}{(i-2)!}$$

$$= (-1)^m m!(i-1).$$

Summing all these terms we get

$$\sum_{i=1}^{m+1}(-1)^m m!(i-1) = (-1)^m m! \binom{m+1}{2}.$$

□

Proof of Theorem 1

Proof. Let $\beta = |\beta|\, e^{i\phi}$, $x \equiv |\beta|$, $M = m_1 + m_2 + m_3 + m_4$, we have

$$
C_{m_1,m_2;m_3,m_4}(\beta) = \sum_n A^*_{n;m_1 m_2} A_{n;m_3 m_4}
$$

$$
= e^{i\phi(m_2+m_3-m_1-m_4)}(-1)^M \sqrt{m_1! m_2! m_3! m_4!}\, x^{-M} e^{-2x^2}
$$

$$
\times \sum_n \frac{x^{4n}}{(n!)^2} \mathcal{L}_{m_1}^{n-m_1}(x^2)\mathcal{L}_{m_2}^{n-m_2}(x^2)\mathcal{L}_{m_3}^{n-m_3}(x^2)\mathcal{L}_{m_4}^{n-m_4}(x^2)
$$

Using the explicit formula for the associated Laguerre polynomial

$$
\mathcal{L}_m^{n-m}(x^2) = \sum_{i=0}^m \frac{1}{i!}\binom{n}{m-i}(-x^2)^i = \sum_{j=0}^m \binom{n}{j}\frac{(-1)^{m-j}}{(m-j)!}x^{2(m-j)},
$$

we find that

$$
\sum_n \frac{x^{4n}}{(n!)^2}\mathcal{L}_{m_1}^{n-m_1}(x^2)\mathcal{L}_{m_2}^{n-m_2}(x^2)\mathcal{L}_{m_3}^{n-m_3}(x^2)\mathcal{L}_{m_4}^{n-m_4}(x^2)
$$

$$
= \sum_{j_1=0}^{m_1}\sum_{j_2=0}^{m_2}\sum_{j_3=0}^{m_3}\sum_{j_4=0}^{m_4}\frac{(-1)^{M-j_1-j_2-j_3-j_4}x^{2(M-j_1-j_2-j_3-j_4)}}{(m_1-j_1)!j_1!(m_2-j_2)!j_2!(m_3-j_3)!j_3!(m_4-j_4)!j_4!}
$$

$$
\times j_1! j_2! j_3! j_4! \sum_n \frac{x^{4n}}{(n!)^2}\binom{n}{j_1}\binom{n}{j_2}\binom{n}{j_3}\binom{n}{j_4}
$$

Letting $z = x^4$, using Lemma 3, we have

$$
j_1! j_2! j_3! j_4! \sum_n \frac{x^{4n}}{(n!)^2}\binom{n}{j_1}\binom{n}{j_2}\binom{n}{j_3}\binom{n}{j_4}
$$

$$
= z^{j_4}\frac{\partial^{j_4}}{\partial z^{j_4}}z^{j_3}\frac{\partial^{j_3}}{\partial z^{j_3}}z^{j_2}\frac{\partial^{j_2}}{\partial z^{j_2}}z^{j_1}\frac{\partial^{j_1}}{\partial z^{j_1}}I_0(2\sqrt{z})
$$

$$
= \sum_{k_4=0}^{j_4}\sum_{k_3=0}^{j_3}\frac{j_4!}{k_4!(j_4-k_4)!}\frac{j_3!}{k_3!(j_3-k_3)!}\frac{j_2!}{(j_2-k_3)!}\frac{(j_2+j_3-k_3)!}{(j_2+j_3-k_3-k_4)!}(\sqrt{z})^{j_1+j_2+j_3+j_4-k_3-k_4}I_{j_1-j_2-j_3-j_4+k_3+k_4}(2\sqrt{z}).
$$

Therefore after some simplification

$$
\sum_n \frac{x^{4n}}{(n!)^2}\mathcal{L}_{m_1}^{n-m_1}(x^2)\mathcal{L}_{m_2}^{n-m_2}(x^2)\mathcal{L}_{m_3}^{n-m_3}(x^2)\mathcal{L}_{m_4}^{n-m_4}(x^2)
$$

$$
= (-1)^M x^{2M}\sum_{j_1=0}^{m_1}\sum_{j_2=0}^{m_2}\sum_{j_3=0}^{m_3}\sum_{j_4=0}^{m_4}\frac{(-1)^{j_1+j_2+j_3+j_4}}{(m_1-j_1)!j_1!(m_2-j_2)!j_2!(m_3-j_3)!j_3!(m_4-j_4)!j_4!}
$$

$$
\times \sum_{k_4=0}^{j_4}\sum_{k_3=0}^{j_3}\frac{j_4!}{k_4!(j_4-k_4)!}\frac{j_3!}{k_3!(j_3-k_3)!}\frac{j_2!}{(j_2-k_3)!}\frac{(j_2+j_3-k_3)!}{(j_2+j_3-k_3-k_4)!}(x^2)^{-k_3-k_4}I_{j_1-j_2-j_3-j_4+k_3+k_4}(2x^2).
$$

Part of the above formula can be further simplified,

$$\sum_{j_3=0}^{m_3}\sum_{j_4=0}^{m_4}\frac{(-1)^{j_3+j_4}}{(m_3-j_3)!j_3!(m_4-j_4)!j_4!}$$

$$\times\sum_{k_4=0}^{j_4}\sum_{k_3=0}^{j_3}\frac{j_4!}{k_4!(j_4-k_4)!}\frac{j_3!}{k_3!(j_3-k_3)!}\frac{j_2!}{(j_2-k_3)!}\frac{(j_2+j_3-k_3)!}{(j_2+j_3-k_3-k_4)!}(x^2)^{-k_3-k_4}I_{j_1-j_2-j_3-j_4+k_3+k_4}(2x^2)$$

$$=\sum_{k_4=0}^{m_4}\sum_{k_3=0}^{m_3}\sum_{j_3=k_3}^{m_3}\sum_{j_4=k_4}^{m_4}\frac{(-1)^{j_3+j_4}}{(m_3-j_3)!(m_4-j_4)!}$$

$$\times\frac{1}{k_4!(j_4-k_4)!}\frac{1}{k_3!(j_3-k_3)!}\frac{j_2!}{(j_2-k_3)!}\frac{(j_2+j_3-k_3)!}{(j_2+j_3-k_3-k_4)!}(x^2)^{-k_3-k_4}I_{j_1-j_2-j_3-j_4+k_3+k_4}(2x^2)$$

$$=\sum_{k_4=0}^{m_4}\sum_{k_3=0}^{m_3}\sum_{j_3=0}^{m_3-k_3}\sum_{j_4=0}^{m_4-k_4}\frac{(-1)^{j_3+k_3+j_4+k_4}}{(m_3-j_3-k_3)!(m_4-j_4-k_4)!}$$

$$\times\frac{1}{k_4!j_4!}\frac{1}{k_3!j_3!}\frac{j_2!}{(j_2-k_3)!}\frac{(j_2+j_3)!}{(j_2+j_3-k_4)!}(x^2)^{-k_3-k_4}I_{j_1-j_2-j_3-j_4}(2x^2)$$

$$=\sum_{k_4=0}^{m_4}\sum_{k_3=0}^{m_3}\frac{(x^2)^{-k_3-k_4}}{k_3!k_4!}(-1)^{k_3+k_4}\frac{j_2!}{(j_2-k_3)!(m_3-k_3)!(m_4-k_4)!}$$

$$\times\sum_{j_3=0}^{m_3-k_3}(-1)^{j_3}\frac{(j_2+j_3)!}{(j_2+j_3-k_4)!}\left(\begin{array}{c}m_3-k_3\\j_3\end{array}\right)\sum_{j_4=0}^{m_4-k_4}(-1)^{j_4}\left(\begin{array}{c}m_4-k_4\\j_4\end{array}\right)I_{j_1-j_2-j_3-j_4}(2x^2).$$

Now

$$\sum_{n}\frac{x^{4n}}{(n!)^2}\mathcal{L}_{m_1}^{n-m_1}(x^2)\mathcal{L}_{m_2}^{n-m_2}(x^2)\mathcal{L}_{m_3}^{n-m_3}(x^2)\mathcal{L}_{m_4}^{n-m_4}(x^2)$$

$$=(-1)^M x^{2M}\frac{1}{m_1!m_2!}\sum_{k_4=0}^{m_4}\sum_{k_3=0}^{m_3}\frac{(x^2)^{-k_3-k_4}}{k_3!k_4!(m_3-k_3)!(m_4-k_4)!}(-1)^{k_3+k_4}$$

$$\times\sum_{j_1=0}^{m_1}(-1)^{j_1}\left(\begin{array}{c}m_1\\j_1\end{array}\right)\sum_{j_2=0}^{m_2}(-1)^{j_2}\left(\begin{array}{c}m_2\\j_2\end{array}\right)\frac{j_2!}{(j_2-k_3)!}$$

$$\times\sum_{j_3=0}^{m_3-k_3}(-1)^{j_3}\frac{(j_2+j_3)!}{(j_2+j_3-k_4)!}\left(\begin{array}{c}m_3-k_3\\j_3\end{array}\right)\sum_{j_4=0}^{m_4-k_4}(-1)^{j_4}\left(\begin{array}{c}m_4-k_4\\j_4\end{array}\right)I_{j_1-j_2-j_3-j_4}(2x^2).$$

We now focus on one term in the double summation $\sum_{k_4=0}^{m_4}\sum_{k_3=0}^{m_3}$, i.e. the summand with fixed k_3 and k_4. It is known that for large z,

$$I_\nu(z)\sim\frac{e^z}{\sqrt{2\pi z}}\left[1-\frac{4\nu^2-1}{8z}+\frac{(4\nu^2-1)(4\nu^2-9)}{2!(8z)^2}+\cdots+(-1)^l\frac{\prod_{i=1}^l\left[4\nu^2-(2i-1)^2\right]}{l!(8z)^l}+\cdots\right],$$

in our case

$$I_{j_1-j_2-j_3-j_4}(2x^2)\sim\frac{e^{2x^2}}{2x\sqrt{\pi}}\left[1-\frac{4(j_1-j_2-j_3-j_4)^2-1}{16x^2}\cdots+(-1)^l\frac{\prod_{i=1}^l\left[4(j_1-j_2-j_3-j_4)^2-(2i-1)^2\right]}{l!(4x)^{2l}}+\cdots\right].$$

The expansion of $I_{j_1-j_2-j_3-j_4}(2x^2)$ contains polynomials of the form $j_1^{p_1}j_2^{p_2}j_3^{p_3}j_4^{p_4}$. Note also $\frac{j_2!}{(j_2-k_3)!}$ is a polynomial of j_2 of degree k_3 and $\frac{(j_2+j_3)!}{(j_2+j_3-k_4)!}$ is polynomial of (j_2+j_3) of degree k_4. So overall the summand of the quadruple summation $\sum_{j_1=0}^{m_1}\sum_{j_2=0}^{m_2}\sum_{j_3=0}^{m_3-k_3}\sum_{j_4=0}^{m_4-k_4}$ is a combination of polynomials of the form $j_1^{p_1}j_2^{p_2}j_3^{p_3}j_4^{p_4}$. Due to Lemma 4, the terms $j_1^{p_1}j_2^{p_2}j_3^{p_3}j_4^{p_4}$ that gives non-zero contribution are those with $p_1\geq m_1$, $p_2\geq m_2$, $p_3\geq m_3-k_3$, and $p_4\geq m_4-k_4$. We try to find such terms with the lowest power in $\frac{1}{x}$. That is to find the smallest l such that the following expression

$$\frac{j_2!}{(j_2-k_3)!}\frac{(j_2+j_3)!}{(j_2+j_3-k_4)!}\prod_{i=1}^l\left[4(j_1-j_2-j_3-j_4)^2-(2i-1)^2\right]$$

contains a term like $j_1^{m_1} j_2^{m_2} j_3^{m_3-k_3} j_4^{m_4-k_4}$ or of even higher order. Since

$$\frac{j_2!}{(j_2-k_3)!}\frac{(j_2+j_3)!}{(j_2+j_3-k_4)!}\prod_{i=1}^{l}\left[4(j_1-j_2-j_3-j_4)^2-(2i-1)^2\right]=j_2^{k_3}(j_2+j_3)^{k_4}4^l(j_1-j_2-j_3-j_4)^{2l}+(\text{lower order terms}),$$

we must require

$$k_3+k_4+2l \geq m_1+m_2+m_3-k_3+m_4-k_4,$$

i.e.

$$2(l+k_3+k_4) \geq m_1+m_2+m_3+m_4 = M.$$

Thus the smallest l should be

$$l_* = \begin{cases} \frac{M}{2}-k_3-k_4, & \text{if } M \text{ even;} \\ \frac{M+1}{2}-k_3-k_4, & \text{if } M \text{ odd.} \end{cases}$$

So if we neglect terms that either gives zero contribution to the quadruple sum over j_i or are not of the leading order in $\frac{1}{x}$,

$$\frac{j_2!}{(j_2-k_3)!}\frac{(j_2+j_3)!}{(j_2+j_3-k_4)!}I_{j_1-j_2-j_3-j_4}(2x^2)$$

$$\sim j_2^{k_3}(j_2+j_3)^{k_4}(-1)^{l_*}\frac{4^{l_*}(j_1-j_2-j_3-j_4)^{2l_*}}{l_*!(4x)^{2l_*}}\frac{e^{2x^2}}{2x\sqrt{\pi}}$$

$$= j_2^{k_3}(j_2+j_3)^{k_4}(j_1-j_2-j_3-j_4)^{2l_*}\frac{(-1)^{l_*}}{l_*!4^{l_*}x^{2l_*}}\frac{e^{2x^2}}{2x\sqrt{\pi}}.$$

When M is even, $2(l_*+k_3+k_4) = M$, so

$$\frac{j_2!}{(j_2-k_3)!}\frac{(j_2+j_3)!}{(j_2+j_3-k_4)!}I_{j_1-j_2-j_3-j_4}(2x^2)$$

$$\sim j_2^{k_3}\sum_{\mu=0}^{k_4}\binom{k_4}{\mu}j_2^{\mu}j_3^{(k_4-\mu)}$$

$$\times(-1)^{m_2+m_3+m_4-2(k_3+k_4)}j_1^{m_1}j_2^{m_2-k_3-\mu}j_3^{m_3-k_3-k_4+\mu}j_4^{m_4-k_4}$$

$$\times\left(\begin{array}{c}M-2k_3-2k_4\\m_1,m_2-k_3-\mu,m_3-k_3-k_4+\mu,m_4-k_4\end{array}\right)\frac{(-1)^{l_*}}{l_*!4^{l_*}x^{2l_*}}\frac{e^{2x^2}}{2x\sqrt{\pi}}$$

$$= (-1)^{M-m_1}\sum_{\mu=0}^{k_4}\binom{k_4}{\mu}\left(\begin{array}{c}M-2k_3-2k_4\\m_1,\ m_2-k_3-\mu,\ m_3-k_3-k_4+\mu,\ m_4-k_4\end{array}\right)j_1^{m_1}j_2^{m_2}j_3^{m_3-k_3}j_4^{m_4-k_4}$$

$$\times\frac{(-1)^{M/2-k_3-k_4}}{(M/2-k_3-k_4)!2^{(M-2k_3-2k_4)}x^{(M-2k_3-2k_4)}}\frac{e^{2x^2}}{2x\sqrt{\pi}},$$

where $\left(\begin{array}{c}n\\k_1,k_2,\cdots,k_m\end{array}\right) \equiv \frac{n!}{k_1!k_2!\cdots k_m!}$.

Using Lemma 4,

$$\sum_{j_1=0}^{m_1}(-1)^{j_1}\binom{m_1}{j_1}\sum_{j_2=0}^{m_2}(-1)^{j_2}\binom{m_2}{j_2}\sum_{j_3=0}^{m_3-k_3}(-1)^{j_3}\binom{m_3-k_3}{j_3}\sum_{j_4=0}^{m_4-k_4}(-1)^{j_4}\binom{m_4-k_4}{j_4}j_1^{m_1}j_2^{m_2}j_3^{m_3-k_3}j_4^{m_4-k_4}$$

$$= \sum_{j_1=0}^{m_1}(-1)^{j_1}\binom{m_1}{j_1}j_1^{m_1}\sum_{j_2=0}^{m_2}(-1)^{j_2}\binom{m_2}{j_2}j_2^{m_2}\sum_{j_3=0}^{m_3-k_3}(-1)^{j_3}\binom{m_3-k_3}{j_3}j_3^{m_3-k_3}\sum_{j_4=0}^{m_4-k_4}(-1)^{j_4}\binom{m_4-k_4}{j_4}j_4^{m_4-k_4}$$

$$= (-1)^{M-k_3-k_4}m_1!m_2!(m_3-k_3)!(m_4-k_4)!.$$

Plugging back to the expression of $\sum_n \frac{x^{4n}}{(n!)^2}\mathcal{L}_{m_1}^{n-m_1}(x^2)\mathcal{L}_{m_2}^{n-m_2}(x^2)\mathcal{L}_{m_3}^{n-m_3}(x^2)\mathcal{L}_{m_4}^{n-m_4}(x^2)$ we eventually get

$$\sum_n \frac{x^{4n}}{(n!)^2}\mathcal{L}_{m_1}^{n-m_1}(x^2)\mathcal{L}_{m_2}^{n-m_2}(x^2)\mathcal{L}_{m_3}^{n-m_3}(x^2)\mathcal{L}_{m_4}^{n-m_4}(x^2)$$

$$\sim (-1)^{m_1+M/2}e^{2x^2}x^{M-1}\frac{1}{2^{M+1}}\frac{1}{\sqrt{\pi}}\sum_{k_4=0}^{m_4}\sum_{k_3=0}^{m_3}\frac{(-1)^{k_3+k_4}2^{2(k_3+k_4)}}{k_3!k_4!(M/2-k_3-k_4)!}$$

$$\times\sum_{\mu=0}^{k_4}\binom{k_4}{\mu}\binom{M-2k_3-2k_4}{m_1,\ m_2-k_3-\mu,\ m_3-k_3-k_4+\mu,\ m_4-k_4}.$$

Finally, we have the leading order contribution for the even M case:

$$C_{m_1,m_2;m_3,m_4}(\beta) \sim x^{-1}e^{i\phi(m_2+m_3-m_1-m_4)}\sqrt{m_1!m_2!m_3!m_4!}(-1)^{m_1+M/2}\frac{1}{2^{M+1}\sqrt{\pi}}$$

$$\times\sum_{k_4=0}^{m_4}\sum_{k_3=0}^{m_3}\frac{(-1)^{k_3+k_4}2^{2(k_3+k_4)}}{k_3!k_4!(M/2-k_3-k_4)!}$$

$$\times\sum_{\mu=0}^{k_4}\binom{k_4}{\mu}\binom{M-2k_3-2k_4}{m_1,\ m_2-k_3-\mu,\ m_3-k_3-k_4+\mu,\ m_4-k_4}$$

$$= \frac{g(m_1,\ m_2,\ m_3,\ m_4,\ \phi)}{|\beta|}.$$

When M is odd, $2(l_*+k_3+k_4)=M+1$. In this case five terms give non-zero contribution under the quadruple sum of j_i, which are $P_1 \equiv j_1^{m_1+1}j_2^{m_2}j_3^{m_3-k_3}j_4^{m_4-k_4}$, $P_2 \equiv j_1^{m_1}j_2^{m_2+1}j_3^{m_3-k_3}j_4^{m_4-k_4}$, $P_3 \equiv j_1^{m_1}j_2^{m_2}j_3^{m_3-k_3+1}j_4^{m_4-k_4}$, $P_4 \equiv j_1^{m_1}j_2^{m_2}j_3^{m_3-k_3}j_4^{m_4-k_4+1}$ and $P_5 \equiv j_1^{m_1}j_2^{m_2}j_3^{m_3-k_3}j_4^{m_4-k_4}$. $P_1, \cdots, P_4$ are the highest order term about the variables j_i in the summand and P_5 is the next highest order. Let us write

$$\frac{j_2!}{(j_2-k_3)!}\frac{(j_2+j_3)!}{(j_2+j_3-k_4)!}I_{j_1-j_2-j_3-j_4}(2x^2) \sim \frac{(-1)^{l_*}}{l_*!4^{l_*}x^{2l_*}}\frac{e^{2x^2}}{2x\sqrt{\pi}}\sum_{\nu=1}^{5}\lambda_\nu P_\nu.$$

The coefficients λ_ν are essentially combinatoric factors and it is not difficult to work them out, although the process can be long and tedious. Eventually we find,

$$\lambda_1 = (-1)^{m_1+1}\sum_{\mu=0}^{k_4}\binom{k_4}{\mu}\binom{M+1-2k_3-2k_4}{m_1+1,\ m_2-k_3-\mu,\ m_3-k_3-k_4+\mu,\ m_4-k_4},$$

$$\lambda_2 = (-1)^{m_1}\sum_{\mu=0}^{k_4}\binom{k_4}{\mu}\binom{M+1-2k_3-2k_4}{m_1,\ m_2-k_3-\mu+1,\ m_3-k_3-k_4+\mu,\ m_4-k_4},$$

$$\lambda_3 = (-1)^{m_1}\sum_{\mu=0}^{k_4}\binom{k_4}{\mu}\binom{M+1-2k_3-2k_4}{m_1,\ m_2-k_3-\mu,\ m_3-k_3-k_4+\mu+1,\ m_4-k_4},$$

$$\lambda_4 = (-1)^{m_1}\sum_{\mu=0}^{k_4}\binom{k_4}{\mu}\binom{M+1-2k_3-2k_4}{m_1,\ m_2-k_3-\mu,\ m_3-k_3-k_4+\mu,\ m_4-k_4+1},$$

$$\lambda_5 = \sum_{\mu=0}^{k_4}\frac{-k_3(k_3-1)}{2}\binom{k_4}{\mu}\binom{M+1-2k_3-2k_4}{m_1,\ m_2-k_3-\mu+1,\ m_3-k_3-k_4+\mu,\ m_4-k_4}$$

$$+\sum_{\mu=0}^{k_4-1}\frac{-k_4(k_4-1)}{2}\binom{k_4-1}{\mu}\binom{M+1-2k_3-2k_4}{m_1,\ m_2-k_3-\mu,\ m_3-k_3-k_4+\mu+1,\ m_4-k_4}.$$

The **key point** to notice is that because $2(l_* + k_3 + k_4) = M + 1$, now the leading term in $\frac{1}{x}$ is

$$\frac{(-1)^{l_*}}{l_*! 4^{l_*} x^{2l_*}} \frac{e^{2x^2}}{2x\sqrt{\pi}} = \frac{(-1)^{(M+1)/2-k_3-k_4}}{((M+1)/2 - k_3 - k_4)! 2^{(M+1-2k_3-2k_4)} x^{(M+1-2k_3-2k_4)}} \frac{e^{2x^2}}{2x\sqrt{\pi}} \sim \frac{1}{x^{(M+1-2k_3-2k_4)}} \frac{e^{2x^2}}{2x\sqrt{\pi}},$$

which is one order higher in $\frac{1}{x}$ compared to the even M case.

Using Lemma 4,

$$\sum_{j_1=0}^{m_1} (-1)^{j_1} \binom{m_1}{j_1} \sum_{j_2=0}^{m_2} (-1)^{j_2} \binom{m_2}{j_2} \sum_{j_3=0}^{m_3-k_3} (-1)^{j_3} \binom{m_3-k_3}{j_3} \sum_{j_4=0}^{m_4-k_4} (-1)^{j_4} \binom{m_4-k_4}{j_4} \sum_{\nu=1}^{5} \lambda_\nu P_\nu$$

$$= (-1)^{M-k_3-k_4} m_1! m_2! (m_3 - k_3)! (m_4 - k_4)!$$

$$\times \left[\lambda_5 + \binom{m_1+1}{2} \lambda_1 + \binom{m_2+1}{2} \lambda_2 + \binom{m_3-k_3+1}{2} \lambda_3 + \binom{m_4-k_4+1}{2} \lambda_4 \right].$$

Now

$$\sum_n \frac{x^{4n}}{(n!)^2} \mathcal{L}_{m_1}^{n-m_1}(x^2) \mathcal{L}_{m_2}^{n-m_2}(x^2) \mathcal{L}_{m_3}^{n-m_3}(x^2) \mathcal{L}_{m_4}^{n-m_4}(x^2)$$

$$\sim (-1)^{(M+1)/2} e^{2x^2} x^{M-2} \frac{1}{2^{M+2}\sqrt{\pi}} \sum_{k_4=0}^{m_4} \sum_{k_3=0}^{m_3} \frac{(-1)^{k_3+k_4} 2^{2(k_3+k_4)}}{k_3! k_4! ((M+1)/2 - k_3 - k_4)!}$$

$$\times \left[\lambda_5 + \binom{m_1+1}{2} \lambda_1 + \binom{m_2+1}{2} \lambda_2 + \binom{m_3-k_3+1}{2} \lambda_3 + \binom{m_4-k_4+1}{2} \lambda_4 \right].$$

Finally,

$$C_{m_1,m_2;m_3,m_4}(\beta) \sim -x^{-2} e^{i\phi(m_2+m_3-m_1-m_4)} \sqrt{m_1! m_2! m_3! m_4!} (-1)^{(M+1)/2} \frac{1}{2^{M+2}\sqrt{\pi}}$$

$$\times \sum_{k_4=0}^{m_4} \sum_{k_3=0}^{m_3} \frac{(-1)^{k_3+k_4} 2^{2(k_3+k_4)}}{k_3! k_4! ((M+1)/2 - k_3 - k_4)!}$$

$$\times \left[\lambda_5 + \binom{m_1+1}{2} \lambda_1 + \binom{m_2+1}{2} \lambda_2 + \binom{m_3-k_3+1}{2} \lambda_3 + \binom{m_4-k_4+1}{2} \lambda_4 \right]$$

$$= \frac{g(m_1, m_2, m_3, m_4, \phi)}{|\beta|^2}.$$

In summary, we have thus proved that for large $|\beta|$,

$$C_{m_1 m_2, m_3 m_4}(\beta) \sim \begin{cases} g(m_1, m_2, m_3, m_4, \phi)/|\beta|, & \sum_{i=1}^4 m_i \text{ is even}; \\ g(m_1, m_2, m_3, m_4, \phi)/|\beta|^2, & \sum_{i=1}^4 m_i \text{ is odd}; \end{cases}$$

NOTE: In fact our technique can be used to prove the general asymptotic result

$$\sum_{n=0}^{\infty} \frac{1}{(n!)^2} x^{4n} \prod_i \mathcal{L}_{m_i}^{n-m_i}(x^2) \sim \begin{cases} x^{\sum_i m_i - 1}, & \sum_i m_i \text{ is even}; \\ x^{\sum_i m_i - 2}, & \sum_i m_i \text{ is odd}. \end{cases}$$

$\square$

[1] D. Gross, Y.-K. Liu, S. T. Flammia, S. Becker, and J. Eisert, Phys. Rev. Lett. **105**, 150401 (2010).

[2] S. T. Flammia, D. Gross, Y.-K. Liu, and J. Eisert, New Journal of Physics **14**, 095022 (2012).

[3] A. Kalev, R. L. Kosut, and I. H. Deutsch, Npj Quantum Information **1**, 15018 EP (2015), article.

[4] G. Tóth, W. Wieczorek, D. Gross, R. Krischek, C. Schwemmer, and H. Weinfurter, Phys. Rev. Lett. **105**,

250403 (2010).

[5] C. Ferrie, Phys. Rev. Lett. **113**, 190404 (2014).

[6] D. H. Mahler, L. A. Rozema, A. Darabi, C. Ferrie, R. Blume-Kohout, and A. M. Steinberg, Phys. Rev. Lett. **111**, 183601 (2013).

[7] M. Cramer, M. B. Plenio, S. T. Flammia, R. Somma, D. Gross, S. D. Bartlett, O. Landon-Cardinal, D. Poulin, and Y.-K. Liu, Nat Commun **1**, 149 (2010).

[8] K. Vogel and H. Risken, Phys. Rev. A **40**, 2847 (1989).

[9] D. Sych, J. Řeháček, Z. Hradil, G. Leuchs, and L. L. Sánchez-Soto, Phys. Rev. A **86**, 052123 (2012).

[10] L. G. Lutterbach and L. Davidovich, Phys. Rev. Lett. **78**, 2547 (1997).

[11] P. Bertet, A. Auffeves, P. Maioli, S. Osnaghi, T. Meunier, M. Brune, J. M. Raimond, and S. Haroche, Phys. Rev. Lett. **89**, 200402 (2002).

[12] B. Vlastakis, G. Kirchmair, Z. Leghtas, S. E. Nigg, L. Frunzio, S. M. Girvin, M. Mirrahimi, M. H. Devoret, and R. J. Schoelkopf, Science **342**, 607 (2013).

[13] M. Hofheinz, H. Wang, M. Ansmann, R. C. Bialczak, E. Lucero, M. Neeley, A. D. O'Connell, D. Sank, J. Wenner, J. M. Martinis, and A. N. Cleland, Nature **459**, 546 (2009).

[14] S. Krastanov, V. V. Albert, C. Shen, C.-L. Zou, R. W. Heeres, B. Vlastakis, R. J. Schoelkopf, and L. Jiang, Phys. Rev. A **92**, 040303 (2015).

[15] R. W. Heeres, B. Vlastakis, E. Holland, S. Krastanov, V. V. Albert, L. Frunzio, L. Jiang, and R. J. Schoelkopf, Phys. Rev. Lett. **115**, 137002 (2015).

[16] M. Mirrahimi, Z. Leghtas, V. V. Albert, S. Touzard, R. J. Schoelkopf, L. Jiang, and M. H. Devoret, New Journal of Physics **16**, 045014 (2014).

[17] Z. Leghtas, S. Touzard, I. M. Pop, A. Kou, B. Vlastakis, A. Petrenko, K. M. Sliwa, A. Narla, S. Shankar, M. J. Hatridge, M. Reagor, L. Frunzio, R. J. Schoelkopf, M. Mirrahimi, and M. H. Devoret, Science **347**, 853 (2015).

[18] Z. Leghtas, G. Kirchmair, B. Vlastakis, R. J. Schoelkopf, M. H. Devoret, and M. Mirrahimi, Phys. Rev. Lett. **111**, 120501 (2013).

[19] N. Ofek, A. Petrenko, R. Heeres, P. Reinhold, Z. Leghtas, B. Vlastakis, Y. Liu, L. Frunzio, S. M. Girvin, L. Jiang, M. Mirrahimi, M. H. Devoret, and R. J. Schoelkopf, nature, accepted (2016).

[20] C. Wang, Y. Y. Gao, P. Reinhold, R. W. Heeres, N. Ofek, K. Chou, C. Axline, M. Reagor, J. Blumoff, K. M. Sliwa, L. Frunzio, S. M. Girvin, L. Jiang, M. Mirrahimi, M. H. Devoret, and R. J. Schoelkopf, Science **352**, 1087 (2016).

[21] B. Calkins, P. L. Mennea, A. E. Lita, B. J. Metcalf, W. S. Kolthammer, A. Lamas-Linares, J. B. Spring, P. C. Humphreys, R. P. Mirin, J. C. Gates, P. G. R. Smith, I. A. Walmsley, T. Gerrits, and S. W. Nam, Opt. Express **21**, 22657 (2013).

[22] S. Haroche and J.-M. Raimond, *Exploring the Quantum: Atoms, Cavities, and Photons* (Oxford University Press, New York, 2006).

[23] M. Brune, F. Schmidt-Kaler, A. Maali, J. Dreyer, E. Hagley, J. M. Raimond, and S. Haroche, Phys. Rev. Lett. **76**, 1800 (1996).

[24] C. Guerlin, J. Bernu, S. Deleglise, C. Sayrin, S. Gleyzes, S. Kuhr, M. Brune, J.-M. Raimond, and S. Haroche, Nature **448**, 889 (2007).

[25] H. Wang, M. Hofheinz, M. Ansmann, R. C. Bialczak, E. Lucero, M. Neeley, A. D. O'Connell, D. Sank, M. Weides, J. Wenner, A. N. Cleland, and J. M. Martinis, Phys. Rev. Lett. **103**, 200404 (2009).

[26] D. Leibfried, D. M. Meekhof, B. E. King, C. Monroe, W. M. Itano, and D. J. Wineland, Phys. Rev. Lett. **77**, 4281 (1996).

[27] S. An, J.-N. Zhang, M. Um, D. Lv, Y. Lu, J. Zhang, Z.-Q. Yin, H. T. Quan, and K. Kim, Nat Phys **11**, 193 (2015), article.

[28] H.-Y. Lo, D. Kienzler, L. de Clercq, M. Marinelli, V. Negnevitsky, B. C. Keitch, and J. P. Home, Nature **521**, 336 (2015), letter.

[29] G. Kirchmair, B. Vlastakis, Z. Leghtas, S. E. Nigg, H. Paik, E. Ginossar, M. Mirrahimi, L. Frunzio, S. M. Girvin, and R. J. Schoelkopf, Nature **495**, 205 (2013).

[30] T. Opatrný and D.-G. Welsch, Phys. Rev. A **55**, 1462 (1997).

[31] S. Mancini, P. Tombesi, and V. I. Man'ko, EPL (Europhysics Letters) **37**, 79 (1997).

[32] S. Deleglise, I. Dotsenko, C. Sayrin, J. Bernu, M. Brune, J.-M. Raimond, and S. Haroche, Nature **455**, 510 (2008).

[33] Unless there are additional constraints to ρ so that other methods like compressed sensing may apply.

[34] J. S. Lundeen, A. Feito, H. Coldenstrodt-Ronge, K. L. Pregnell, C. Silberhorn, T. C. Ralph, J. Eisert, M. B. Plenio, and I. A. Walmsley, Nat Phys **5**, 27 (2009).

[35] L. Zhang, H. B. Coldenstrodt-Ronge, A. Datta, G. Puentes, J. S. Lundeen, X.-M. Jin, B. J. Smith, M. B. Plenio, and I. A. Walmsley, Nat Photon **6**, 364 (2012).

[36] Actually, in some experiments the Wigner function was obtained from Q_n^β [13, 29].

[37] Z. Leghtas, G. Kirchmair, B. Vlastakis, M. H. Devoret, R. J. Schoelkopf, and M. Mirrahimi, Phys. Rev. A **87**, 042315 (2013).

[38] A. I. Lvovsky, Journal of Optics B: Quantum and Semiclassical Optics **6**, S556 (2004).

[39] R. Bhatia, *Matrix Analysis* (Springer-Verlag, New York, 1997).

[40] Y. I. Bogdanov, G. Brida, M. Genovese, S. P. Kulik, E. V. Moreva, and A. P. Shurupov, Phys. Rev. Lett. **105**, 010404 (2010).

[41] A. Miranowicz, K. Bartkiewicz, J. Peřina, M. Koashi, N. Imoto, and F. Nori, Phys. Rev. A **90**, 062123 (2014).

[42] A. Miranowicz, i. m. c. K. Özdemir, J. c. v. Bajer, G. Yusa, N. Imoto, Y. Hirayama, and F. Nori, Phys. Rev. B **92**, 075312 (2015).

[43] M. Grant and S. Boyd, "CVX: Matlab software for disciplined convex programming, version 2.1," `http://cvxr.com/cvx` (2014).

[44] M. Grant and S. Boyd, in *Recent Advances in Learning and Control*, Lecture Notes in Control and Information Sciences, edited by V. Blondel, S. Boyd, and H. Kimura (Springer-Verlag Limited, 2008) pp. 95–110, `http://stanford.edu/~boyd/graph_dcp.html`.

[45] W. Chen, J. Hu, Y. Duan, B. Braverman, H. Zhang, and V. Vuletić, Phys. Rev. Lett. **115**, 250502 (2015).